ISSN No:-2456-2165 https://doi.org/10.38124/ijisrt/IJISRT24SEP1537

Computational Exploration of Variable-Pitch Fans as Thrust Reversers and Their Influence on Noise Abatement in Turbofan Propulsion Systems

Mahdi Hossein Gholi Nejad[1]; Mofid Gorji Bandpy[2]
Babol Noshirvani University of Technology

Abstract:- Variable pitch propellers, once confined to turboprop engines, are now revolutionizing turbofan applications. Recent breakthroughs in materials and technology, exemplified by Pratt & Whitney's geared turbofan engine, underscore the practicality of variable pitch systems. Ongoing research promises to extend their adoption across diverse engine types, significantly enhancing safety and performance. This study investigates a novel approach to enhance reverse thrust using dual-row radial fans with adjustable pitch angles. These fan blades exhibit geometry variations, combining features from both turbofan motor fan blades and turbo-propeller motor blades. The results are promising: this configuration nearly triples the thrust force, producing approximately 292.917 kilo-newtons. Moreover, it enables the generation of reverse thrust equivalent to 25.077 kilo-newtons. These enhancements are achieved while reducing blade rotational speed from 5200 revolutions per minute to 3200 revolutions per minute and inlet airspeed from 660 km/h (at maximum power) to 220 km/h. Additionally, a notable 11% reduction in noise level at the blade tips has been observed. This research sheds light on the potential of innovative fan blade designs to revolutionize reverse thrust capabilities in turbofan engines, contributing to safer and more efficient aircraft landings.

Keywords:- *Reverse Thrust; Noise Mitigation; Computational Fluid Dynamic; Braking System; Pitch Angle.*

I. INTRODUCTION

Modern aviation hinges on a delicate interplay between technology and physics during the critical landing phase. As an aircraft gracefully touches down on the runway, achieving rapid deceleration to a safe speed becomes paramount. This intricate dance necessitates a harmonious blend of traditional wheel brakes and an ingenious system known as reverse thrust. An overview of current reverse thrust systems including cascade type reverse, clam shell door and bucket target system are shown in figure1. While these reverse thrust mechanisms dutifully serve their purpose, they carry inherent drawbacks:

➢ *Increased Weight and Complexity:*

The intricate machinery adds weight and complexity, impacting overall aircraft performance.

➢ *Engine Wear Considerations:*

Frequent use of reverse thrust can accelerate wear on critical engine components.

➢ *Noise Levels:*

The cacophony generated during reverse thrust maneuvers poses challenges for noise-sensitive environments.

This groundbreaking research introduces a novel approach: a meticulously designed inlet fan. This fan features concentric blades—the inner blade supplies air to the engine core, while the outer blade cools the bypass duct. By dynamically adjusting the pitch of the outer blade, we unlock the ability to generate reverse thrust. The proposed approach offers several compelling advantages over traditional systems:

- *Lightweight and Streamlined:*

✓ Reduced complexity translates to a lighter overall system.

- *Enhanced Efficiency:*

✓ Optimized airflow leads to improved fuel efficiency.
- *Quieter Landings:*

✓ Reduced noise impact during reverse thrust maneuvers.
- *Mitigated Engine Wear:*

✓ Minimized stress on critical engine components.

ISSN No:-2456-2165 https://doi.org/10.38124/ijisrt/IJISRT24SEP1537

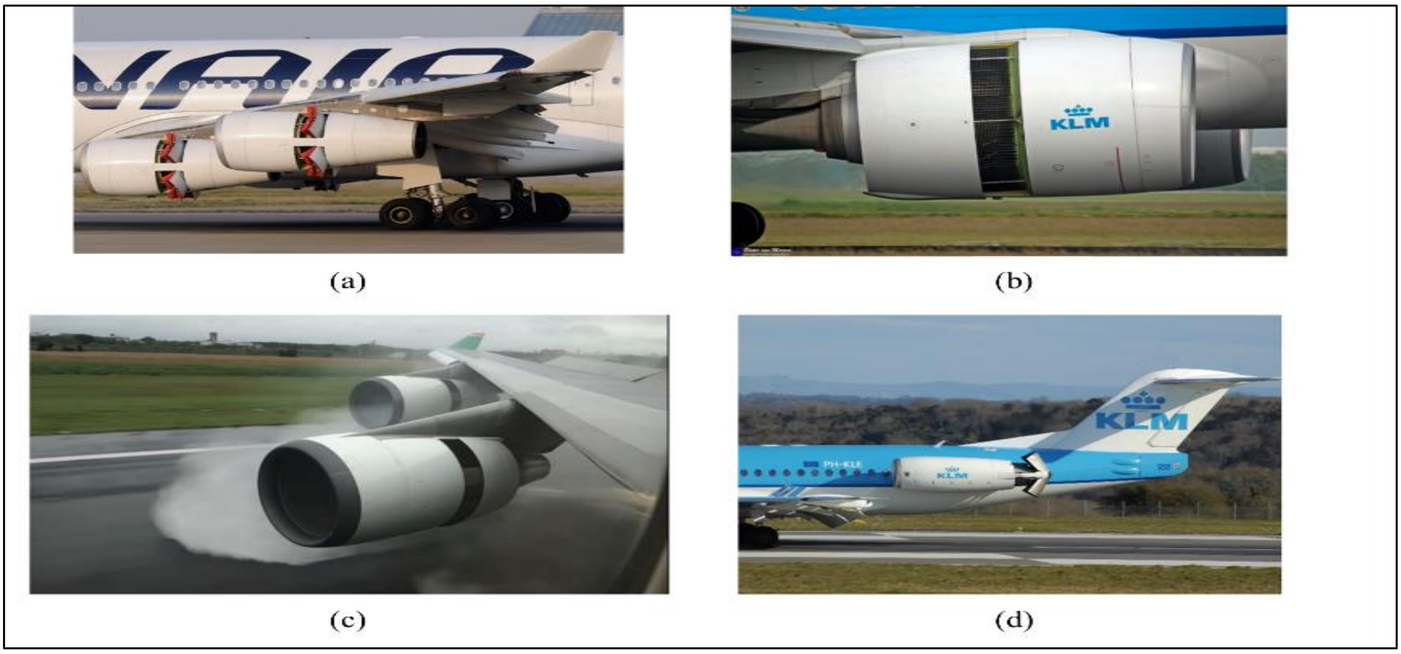

Fig 1 Types of Modern Reverse Thrust Systems: (a) Reverse thrust using hot and cold gas before nozzle exit (b) Reverse thrust using cool bypass air from the fan (c) Reverse thrust using the cascade technique during a rainy landing (d) Using the hot and cold gas after nozzle exit with deflection doors

Variable pitch propellers, once confined to turboprop engines, are now gaining traction in turbofan applications. Recent strides in materials and technology, epitomized by Pratt & Whitney's geared turbofan engine, underscore the practicality of variable pitch systems. Ongoing research promises to extend their adoption across diverse engine types, enhancing both safety and performance. Variable pitch propellers offer a significant edge over fixed pitch counterparts, making them indispensable for various applications. Their adaptability—allowing precise blade angle adjustments across different flight phases—translates into substantial benefits. During takeoff, aggressive pitch angles maximize thrust, while gradual reduction optimizes cruise efficiency. This adaptability ensures peak engine performance, curbing fuel consumption and emissions. Moreover, variable pitch propellers play a pivotal role in enhancing aircraft safety and maneuverability. The ability to fine-tune pitch angles facilitates better deceleration control during landings. By reversing blade pitch, these propellers create reverse thrust, shortening landing distances and enhancing overall braking performance. Additionally, they improve acceleration during takeoff and maneuverability during flight.

A variable-pitch fan engine was evaluated in the Ames wind tunnel by Reemsnyder [3] to assess forward velocity and crosswind effects on reverse-thrust performance. Two inlet configurations were assessed, and a flared fan nozzle was utilized for reverse-thrust operations. Steady-state reverse-thrust performance was observed up to 54 m/s. A significant drop in reverse thrust was noted at approximately 30 m/s. Reverse thrust was achieved after transitioning from forward to reverse thrust both statically and up to 30 m/s. Short-haul aircraft require effective deceleration from speeds around 40 m/s or greater. During deceleration, consistent thrust reversal is essential to mitigate yawing from uneven thrust levels. Forward velocity led to unexpected partial reverse thrust steady-state operation under certain conditions. Complete or partial reverse thrust was only achievable after forward-to-reverse thrust transients at velocities up to about 30 m/s. These negative impacts of forward velocity may be specific to this fan-nacelle configuration. The Q-Fan T-55 demonstrator engine featured a low-pressure ratio and a simplistic conical exlet. The findings may not be representative of higher-pressure ratio fans. Additionally, no modifications were made to the nacelle to alleviate the negative impacts of forward velocity. Continued development of advanced variable-pitch turbofan engines is thus advocated to ensure reliable reverse-thrust levels for effective aircraft deceleration.

Hall et al [4] investigates the 3D flow field of variable pitch fans operating in reverse thrust mode for low-pressure ratio fan systems. Using the Advanced Ducted Propulsor variable pitch fan test case with a design fan pressure ratio of 1.29, the research validates its computational approach against spanwise probe measurements in forward thrust before extending the method to reverse thrust configurations. The analysis, conducted at two rotor stagger settings, reveals poor alignment between the spanwise variation in relative flow angle and the rotor inlet metal angle, resulting in two main rotor loss sources: positive incidence at the tip and negative incidence at lower span fractions. Opening the rotor stagger setting reduces the latter loss but increases the former at higher rotor suction surface Mach numbers. While more open rotor settings yield higher mass flow and gross thrust (up to 49% of forward take-off value), they are limited by increased losses at high speeds. This research contributes to understanding the potential of variable pitch fans in eliminating the need for bypass duct thrust reversers, potentially reducing engine drag and weight.

ISSN No:-2456-2165 https://doi.org/10.38124/ijisrt/IJISRT24SEP1537

Moreno et.al [5] investigates the potential of counter-rotating turbofan (CRTF) engines to meet future aviation demands for reduced fuel consumption, emissions, and noise. Using a Blade Element Method (BEM) and semi-empirical noise models, the research compares a baseline GE90 engine with two CRTF configurations: one with similar fan pressure ratio (FPR) and another with higher FPR. The analysis focuses on specific fuel consumption, emissions, and noise levels during takeoff. Results indicate that CRTFs can potentially reduce noise levels by approximately 3 EPNdB compared to the baseline, with minimal improvements in thrust-specific fuel consumption (TSFC) for higher FPR configurations. The study highlights the need for adapted noise models to capture rotor-rotor interaction tones and suggests implementing more comprehensive takeoff profiles for future research.

This study investigates the performance of a full-size, variable-pitch-fan engine designed for future short-haul aircraft, focusing on rapid forward-to-reverse-thrust transitions. The research encompassed approach-power thrust reversals through feather-pitch and flat-pitch modes, as well as aborted-takeoff transients, using both bellmouth and flight inlets. Results demonstrate that rapid approach-power thrust reversals can be achieved without significant engine limitations, with response times of approximately 1.0 second. The study identified fan stall issues during through-feather-pitch operation with a flight inlet, which were mitigated using a blade "overshoot" technique. While high fan blade vibratory stresses were observed during through-feather-pitch transitions, they remained within acceptable limits. The research concludes that variable-pitch fans offer a promising solution for rapid reverse-thrust capability in future short-haul aircraft. [6]

Steffen et al in their study investigated the reverse-thrust performance of hemispherical target-type thrust reversers using small-scale models with unheated air. The research found that hemisphere diameter was the most critical factor in increasing reverse-thrust ratio, with a maximum of 82% achieved using a 1.8-closed-nozzle-diameter hemisphere. Positioning the reverser close to the nozzle and slightly opening the exhaust nozzle improved performance for some configurations. High reverse-thrust ratios required turning the flow close to the boattail, with attached flow on the boattail contributing up to 20% of the reverse-thrust ratio. Boattail shape variations generally had minimal impact on performance. The study also found that a reverser made from a spherical or cylindrical surface and a flat plate performed satisfactorily and might offer advantages in stowage and jet directional control compared to fully hemispherical designs. The research provides insights into optimizing thrust reverser geometry for improved aircraft deceleration capabilities. [7]

Moreno and Martinez [8] study examines the potential of counter-rotating turbofan (CRTF) engines to address the aviation industry's challenges of rising fuel costs and stricter noise regulations. Using a Blade Element Method (BEM) and semi-empirical noise models, the research compares a baseline GE90 engine with two counter-rotating fan (CRF) configurations: one with similar properties but lower rotational speed, and another with higher fan pressure ratio (FPR). The analysis focuses on specific fuel consumption, emissions, and noise levels. Results indicate that CRFs can potentially reduce the equivalent perceived noise level (EPNL) compared to the baseline single-stage arrangement, with similar reductions in other noise descriptors. The study suggests that CRTFs may offer a revolutionary solution to meet the ambitious objectives set by the Advisory Council for Aeronautics Research in Europe (ACARE) for 2020, potentially improving both fuel efficiency and noise performance in future aircraft engines.

Saiyed et al [9] in their study investigates the acoustic and flow characteristics of a scale-model cascade thrust reverser. The research compares forward and reverse thrust conditions, focusing on pressure distributions and sound pressure levels (SPL). In forward thrust, inner barrel static pressure distributions and acoustic spectra remain largely constant. However, reverse thrust conditions show significant changes, including adverse pressure gradients leading to flow deceleration and separation on the inner barrel, and favorable pressure gradients causing flow acceleration on the blocker door. The study observes substantial SPL amplification in areas of axial flow deceleration and radial flow acceleration during reverse thrust. These findings contribute to understanding the mechanisms behind increased noise levels in reverse thrust operations, utilizing hardwall reflection and vortex stretching theories to explain the observed phenomena.

Atassi and Logue [10] in their study investigates the broadband noise generation in the fan rotor of a high bypass ratio turbofan engine using numerical analysis of unsteady aerodynamics. The research examines cruise and takeoff conditions, each at three operating points: normal, choked, and near-surge. The study identifies three primary broadband noise mechanisms: interaction of incoming flow turbulence with the engine casing and nose, interaction of turbulent boundary layers on rotor blades with their trailing edges, and interaction of rotating blades with incoming flow turbulence. The trailing edge interaction emerges as the most significant noise source. The choked condition produces the highest noise levels due to maximum turbulent kinetic energy, mass flow rate, and relative Mach number. Conversely, the near-surge condition generally exhibits the lowest noise levels, except for increased noise on the lower suction side of the rotor caused by reverse flow and vortices. This research contributes to understanding and predicting fan noise in various operating conditions of turbofan engines.

Rao et al [11] investigates the installed flow field of a Variable Pitch Fan (VPF) operating in reverse thrust during aircraft landing. The research develops a VPF design for a 40,000 lbf modern high bypass ratio engine and creates a comprehensive engine model including nacelle, core components, and bypass structures. The model is integrated with a representative airframe in landing configuration and a rolling ground plane to simulate realistic conditions. Using 3D RANS solutions, the study examines the flow field for different VPF stagger angles and rotational speeds. The analysis reveals a complex interaction between free stream and reverse stream flows, forming a shear layer in fan passages that deflects radially outward before turning back. The flow field characteristics vary with stagger setting, fan speed, and aircraft landing speed due to changes in stream momentum. This research provides crucial insights for qualifying VPF designs and optimizing operating settings during different stages of aircraft landing, addressing limitations in typical uninstalled static flow field designs.

Rao et al [12] in another study investigates the necessary model fidelity for accurately assessing the feasibility of using Variable Pitch Fans (VPF) in modern high bypass ratio aero engines for reverse thrust generation. The research compares 3D RANS flow field solutions from two models: an isolated engine model and an integrated model with the engine installed on an airframe in landing configuration. Results at 80 knots landing speed reveal significant differences between the models in reverse stream quantity, circumferential flow property distribution, and downstream flow development. The isolated model overestimates reverse stream mass flow by 74%, reverse thrust by 66%, and radial distortion index (RDI) by 61%, while underestimating circumferential distortion index (CDI) by 79%. The study concludes that an integrated model is essential for accurate representation of the VPF reverse thrust flow field, as it captures crucial interactions between the engine, airframe, and ground effects. This comprehensive approach is recommended for making informed engineering decisions in VPF system design and overall aircraft optimization.

Rostamalizadeh [13] discussed thrust reverser mechanisms in aviation, focusing on their role in providing additional braking during aircraft landing. Three types of thrust reversers are examined: cascade type, clamshell door system, and bucket target system. The bucket target system is highlighted for its advantages and efficiency. The authors emphasize the importance of this technique in improving safety, especially in adverse weather conditions, and in utilizing energy that would otherwise be wasted. They conclude that placing the thrust reverser at the nozzle exit, where maximum thrust is available, is most effective, with the bucket target type being particularly efficient due to its ability to reverse the maximum amount of thrust using deflector doors at the rear of the jet engine.

Smith et al [14] conducted that high-bypass-ratio aero-engines increase wing-engine interference, affecting nacelle design. This CFD study analyzes aircraft/engine integration with reverse cascade thrust. Wing lift coefficient decreases 21.2% and 45.02% as the engine moves forward horizontally by 11%L and 21.2%L, respectively. Vertical engine movement of -3.5%L and 3.5%L reduces lift by 2.4% and 4.82%. Reverser airflow is less constrained without airframe interference. Reverse thrust efficiency decreases as the engine nacelle moves from baseline, especially forward horizontally. Results highlight complex interactions between engine positioning and aerodynamic performance in modern aircraft designs.

Zhang et al [15] study employs three-dimensional Reynolds-averaged Navier-Stokes equations to analyze the reverser flow field of a business jet during landing under various taxiing velocities. The research compares single engine and aircraft/engine integrated models, revealing that the reverser flow's influence range expands as landing speed decreases, potentially leading to re-inhalation. The integrated model shows asymmetrical reverser flow due to fuselage and wing interference, unlike the single engine model. Adjusting the engine nacelle position affects both incoming and reverser airflows, with forward and upward movement improving reverser effect but potentially increasing fuselage surface noise. The study demonstrates that a 17% forward extension of the nacelle results in lower noise levels compared to an 11% extension, and downward movement generates less noise than upward movement. These findings contribute to understanding the complex interactions between reverser flow, aircraft geometry, and engine positioning during landing operations.

Mishra et al [16] investigate the optimal aerofoil blade profile for axial flow mine ventilation fans to improve energy efficiency. Using ANSYS Fluent 6.3.26 CFD simulations, six typical aerofoil sections were analyzed at angles of attack from 0° to 21° at 3° intervals, with a Reynolds number of 3 × 10^6. The research examined lift (Cl) and drag (Cd) coefficients as functions of angle of attack (α) to assess aerofoil efficiency. Results showed that angle of attack significantly affects lift and drag coefficients, with stall conditions occurring at α values of 12° and 15° for most aerofoils. The study identified the most efficient blade profile based on the highest lift-to-drag ratio (Cl/Cd). This research provides a foundation for selecting appropriate blade profiles for axial flow fans in the mining industry, potentially leading to improved energy efficiency and cost savings in mine ventilation systems.

Varsegov et al [17] on their study presents a numerical model for flow analysis in a cascade-type thrust reverser of a turbofan engine, specifically designed for the bypass duct of the advanced PD-14 gas-turbine engine. The research focuses on simulating viscous compressible single-phase flow in the bypass duct and interblade space of the thrust reverser cascade. The authors investigated the impact of different turbulence models on calculation results, comparing them with experimental data obtained from a thrust reverser model. The study utilized a 1:2 scale model of the thrust reverser cascade, featuring aerofoil blades with a constant incidence angle of 50 degrees. By identifying an optimal turbulence model for this flow type and verifying the numerical model against experimental results, the research contributes to the understanding and design optimization of cascade-type thrust reversers in turbofan engines.

Schrantz et al [18] presents a novel variable pitch fan system design for high bypass turbofan engines, offering 10-14% fuel savings for next-generation engines. The design features a compact pitch change mechanism within the fan's center body, utilizing multiple high-strength tension/torsion straps to support blade centrifugal loads while allowing 10-15 degrees of blade pitch rotation. This system balances blade

ISSN No:-2456-2165 https://doi.org/10.38124/ijisrt/IJISRT24SEP1537

centrifugal twisting loads with strap restoring moments, reducing pitch control forces and enabling on-wing blade replacement through a pin root design. The variable pitch capability eliminates the need for a variable area nozzle to prevent fan stall flutter, resulting in weight, complexity, and cost savings. The design, which is progressing with patents and scaled model fabrication, employs advanced materials like carbon fiber with thermoplastic resin for the tension/torsion straps. This innovative approach provides a robust, scalable, and cost-effective solution for significantly improving turbofan engine efficiency while maintaining comparable weight to current fan systems.

Wang et al [19] presents initial research on modeling the evolution of product families and the rationale behind their changes, a strategy employed by manufacturing companies to offer product variety while reducing development costs. The proposed information model, an extension of the NIST Core Product Model, comprises three submodels: Product Family, Family Evolution, and Evolution Rationale. The study introduces a Unified Modeling Language (UML)-based representation of this conceptual model and describes a prototype implementation. By providing a framework to capture and represent the evolution of product families and the reasoning behind design changes, this research aims to support manufacturers in managing product diversity efficiently and understanding the developmental trajectory of their product lines. This approach could potentially lead to more informed decision-making in product development and improved strategies for maintaining competitive product portfolios.

Zhang et al [20] examines the aerodynamic performance of a cascade within a cold stream thrust reverser, a key component in aircraft power plant systems. Using realistic operating conditions, the research conducts aerodynamic simulations on three idealized cascade models representing different design options. The primary objectives are to improve the cascade's aerodynamic performance while minimizing weight and, notably, to incorporate noise reduction considerations into the thrust reverser design for the first time. Results show that while the weight-reduced designs (5% and 10%) slightly decrease total reverse thrust, they successfully eliminate the supersonic flow regime present in the original design. This leads to improved aerodynamic performance around the cascade and within the fan duct, as well as enhanced acoustic characteristics. The study demonstrates that significant improvements in flow characteristics and noise reduction can be achieved without substantially compromising the total reverse thrust, offering potential advancements in thrust reverser design for modern aircraft.

In summary, this innovative reverse thrust approach and the resurgence of variable pitch propellers herald a safer and more efficient era for aviation. While further research and prototyping remain essential, the trajectory is clear: safer landings are within reach.

Variable pitch propellers, despite their significant advantages, come with specific limitations and necessitate additional considerations when compared to fixed pitch propellers. These include:

➢ *Increased Complexity:*

- The mechanism enabling variable pitch introduces additional intricacy to the propeller system.
- This complexity may lead to more frequent maintenance requirements and potentially higher lifecycle costs.

➢ *Control System Requirements:*

- Variable pitch propellers require a dedicated control system to adjust blade pitch during flight.
- However, this control system adds weight and complexity to the overall aircraft design.

➢ *Manufacturing Complexity:*

- The design and manufacturing of variable pitch propellers can be more intricate than that of fixed pitch propellers.
- Consequently, initial acquisition costs may be impacted.

Fan blade opening design is determined by several factors, including engine size, airflow requirements, operating conditions, and aerodynamic efficiency goals. The aperture must be optimized to ensure proper aerodynamic performance and minimum blade weight while meeting the engine's cooling or thrust requirements. The proposed concept consists of two parts:

- *Inner Blades:*
  These are connected to the hub and nose of the engine.

- *Outer Blades:*
  These are connected to a shroud that can extract energy and rotation from the central axis, or even be controlled separately.

The purpose of this two-part design is to reduce fan noise and utilize a force called reverse thrust as a braking force during landing.

Excessive fan noise is a problem with conventional fan designs. It is primarily caused by the use of long blades to increase thrust. Modern engineers have proposed an alternative solution: increasing the width of the blades instead of their height. This improves thrust while also reducing fan noise. This type of fan design has not yet been fully commercialized due to its high technological complexity. It has only been implemented in a limited number of engines, including the General Electric GE90-115B engine. This engine is considered a masterpiece of engineering and is used in the Boeing 777-200LR and 777-300ER aircraft, producing a thrust of 93,700 pounds (416.8 kN). To better understand the evolution of fan design, Figure 2 compares the fans of two turbofan engines: the GE90-94B and the CFM56-7B-27. The images clearly show the change in design patterns from the past to the present.

ISSN No:-2456-2165
https://doi.org/10.38124/ijisrt/IJISRT24SEP1537

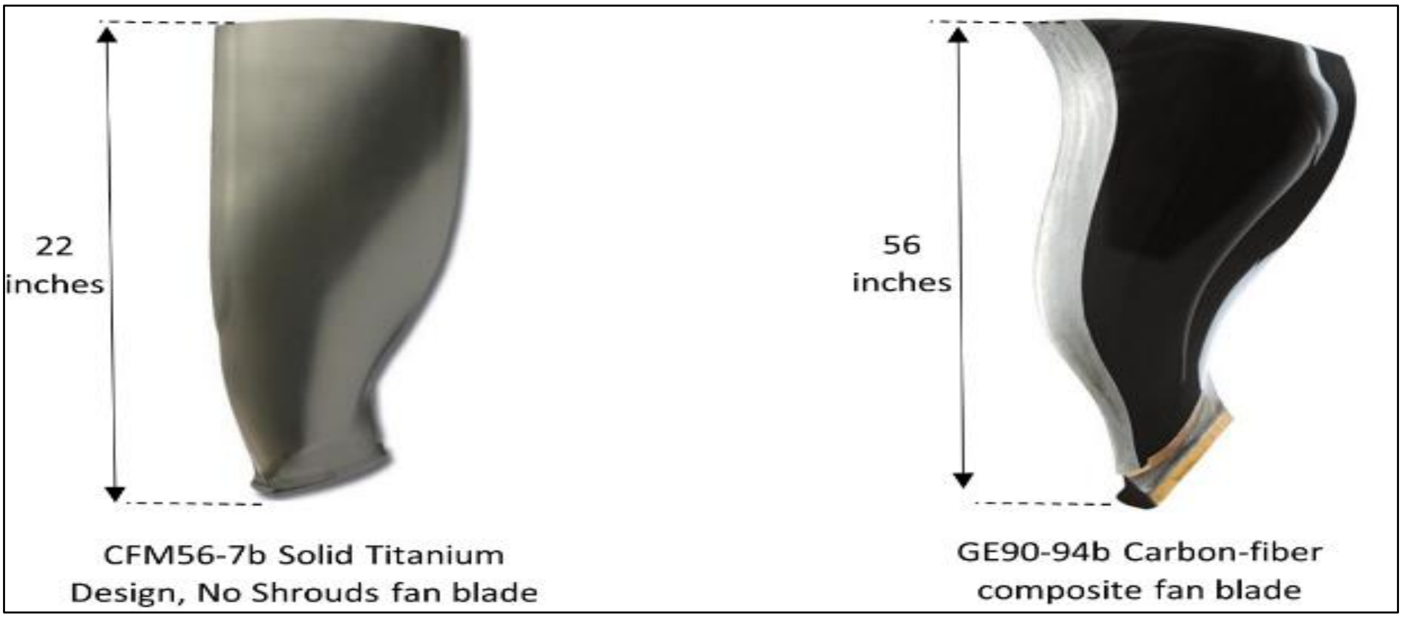

Fig 2 Comparison of Dimensions and Design of Fan Blades from Two Powerful Motors from General Electric and CFM

The proposed VPF [3]concepts offer several advantages over conventional fan designs, including reduced noise, improved efficiency, and enhanced reverse thrust capabilities. Further research and development are needed to fully commercialize these concepts and realize their potential benefits.

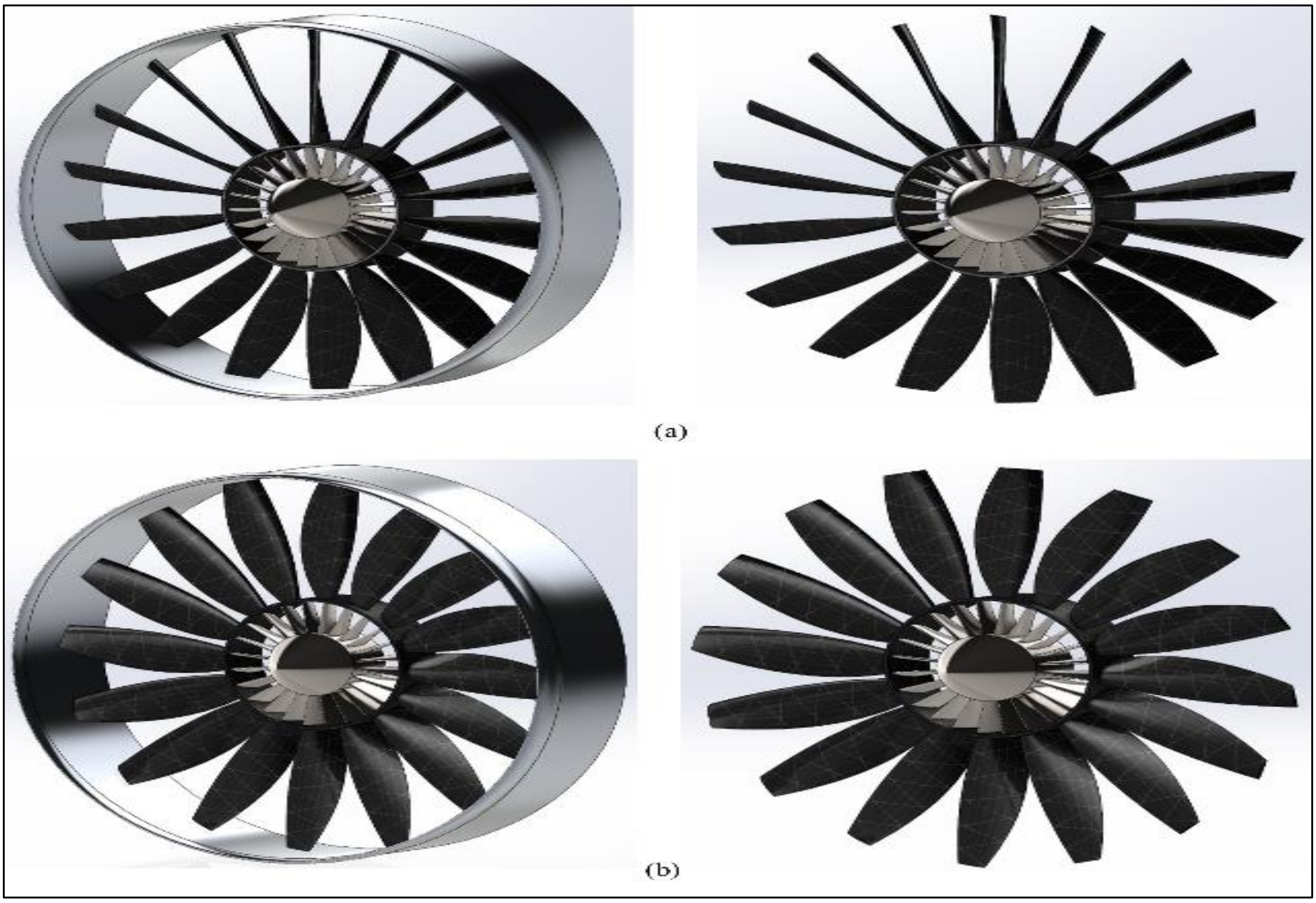

Fig 3 The drawn models for the Proposed Geometry (a) Pitch Angle of 90 Degrees at the Root
(b) Pitch Angle of 29.5 Degrees at the Root

[3] Variable Pitch Fan

ISSN No:-2456-2165 https://doi.org/10.38124/ijisrt/IJISRT24SEP1537

The proposed geometry includes a set of fan blades in the internal fan and propeller blades whose design originates from propeller engines as the outer fan (external fan). This plan will be designed and examined in two different vane angles so that these two vane angles are equivalent to soft and reverse modes in propeller engines. An important point in the design of propellers in propeller engines is that to change the flight mode from the smooth mode (where the airfoils of different sections of the blades are almost horizontal) to the reverse mode (the airfoils in the propeller sections are in such a way that they are almost perpendicular to the axis of rotation) passing blades), experience a large blade angle change, typically greater than 90 degrees, which somewhat negates the efficiency of the in-flight pitch angle change system to produce reverse thrust when needed (such as braking force). This large change in the pitch angle of the propellers can be attributed to the linearity of the profile of the blades.

The propeller will suffer some twisting at the base of the propeller blades, but this change in propeller length is a maximum of 20 degrees for propellers with a diameter greater than 2.5 meters (typically 15 degrees for propellers with a diameter of 2.03 meters and smaller), which is not It is uniformly distributed throughout the propeller and is most concentrated at the base of the propeller blade, although this amount of twist angle is lower than that found in today's turbofan fan blade designs (implemented across the blade axis). According to what mentioned so far, the geometry of the proposed design aims to combine what is used in the blades of turboprop engines and the fans of turbofan engines. The geometries drawn in the SolidWorks software related to this design are shown in the figure in two different pitch angles that obtain two soft and reverse modes in the engine, respectively. The value of the pitch angle in the second state changes by +60.5 degrees compared to the first state.

The height of the propeller blades in this geometry is the same as the geometry of the first design and is equal to 798 mm. The blades of this fan are distributed in 8 sections that are placed at equal distances along the axis of the blade. Three series of asymmetric airfoils from the family of NASA series 4 airfoils have been used. The details of the airfoils used in this geometry are categorized and visible in Figure (5) and Table (1).

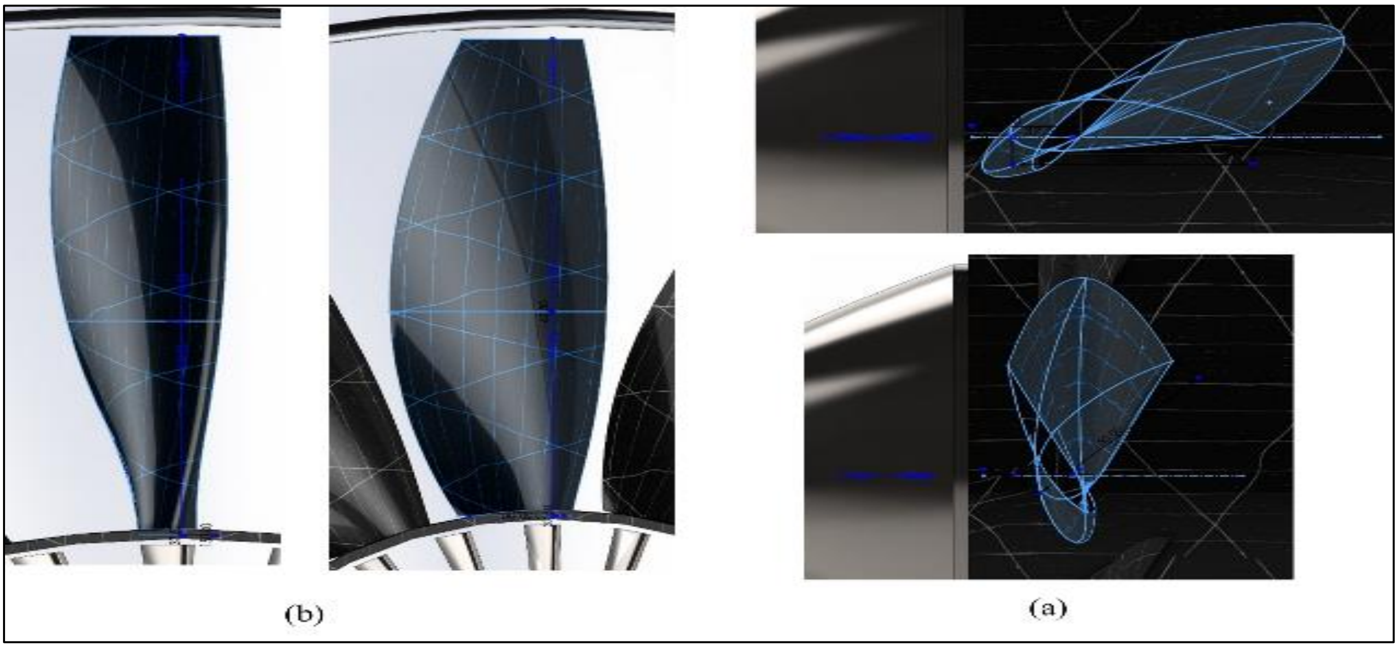

Fig 4 How to change the pitch angle of the fan blades of the second row in the geometry of design 2 (a) top view from top to bottom corresponding to the pitch angle of 90 and 29.5 degrees (b) front view from right to left respectively corresponding to the pitch angle of 90 and 29.5 degrees

The reasons for choosing NACA 84-30, NACA 64-12 and NACA 12-44 airfoils for the design of variable pitch vanes in turbofan engines with the second design geometry:

The NACA 84-30 airfoil is chosen for the root areas of the blades because its high thickness produces a lot of thrust. Also, its short chord length reduces the noise caused by the blade.

The NACA 64-12 airfoil is chosen for the middle areas of the blades because its medium thickness creates a good balance between thrust and drag. Also, its variable chord length reduces the noise caused by the blade.

The NACA 44-12 airfoil is chosen for the tip areas of the blades because its low thickness reduces the drag force. Also, its long chord length increases the thrust force.

Airfoil selection conditions for optimal design in order to produce thrust and reverse thrust as well as reduce noise caused by fan blades.

Table 1 Characteristics of Different Cross-Sections of External Fan Blades of the Second Geometry and Blade Angles of Airfoils used in Two modes of Soft Flight and Reverse Propulsion.

Chord Length (mm)	Blade angle (Reverse Thrust)	Blade angle (Feather)	Airfoil Type	The distance from the blade root as a percentage of the length (%)
150	29.5	90	NACA 84-30	0
180.3	19.38	79.88		14.29
216.7	8.853	70.353	NACA 64-12	28.57
250	1.331	61.831		42.86
225	-6.027	54.473	NACA 44-12	57.14
200	-12.249	48.251		71.43
175	-17.464	43.036		85.71
150	21.829	38.671		100
Blade Height: 798 mm				
Blade No.: 16				

Table 2 Performance Comparison of Selected Airfoils for the Second Design with Airfoils of the same Family

Characteristic		Blade-Induced Noise	Performance at Low Speeds	Performance at High Speeds	Drag Coefficient	Thrust Force	Aerodynamic Shape	Chord Length	Thickness
NACA 84-30		High	Excellent	Good	High	High	Streamlined	Short	High
NACA 64-12		Medium	Good	Good	Medium	Medium	Symmetrical	Variable	Medium
NACA 44-12		Low	Poor	Poor	Low	Low	Wide	Long	Low
Other NACA Series Airfoils	8230, 8630, 9030	High	Excellent	Good	High	High	Symmetrical	Variable	-
	2412,2612 ,2812	High	Poor	Good	Low	High	Symmetrical	Variable	-

ISSN No:-2456-2165 https://doi.org/10.38124/ijisrt/IJISRT24SEP1537

➢ *In the Optimal Design of Variable Pitch Vanes, the following Factors should be Considered:*

- Thrust: The airfoil must produce enough thrust to meet the needs of the aircraft.
- Drag coefficient: the airfoil should have a low drag coefficient to reduce the fuel consumption of the aircraft.
- Performance at high and low speeds: The airfoil must perform well at high and low speeds.
- Blade noise: Airfoils should reduce blade noise to increase passenger comfort.

According to these factors, NACA 84-30, NACA 12-64 and NACA 12-44 airfoils are the right choice for designing variable pitch vanes in turbofan engines. These airfoils have a combination of the following advantages:

- High thrust
- Low drag coefficient
- Good performance at high and low speeds
- Reduction of noise caused by the blade

Of course, choosing the right airfoil for the design of variable pitch blades also depends on other factors, such as the type of engine, the flight speed of the aircraft and the weight of the aircraft. It led to the desired and optimal final result. In the table below, the results of the performance of several replacement airfoils with the selected airfoils are shown in a comparative manner.

In order to measure the performance of the proposed design, or more generally, whether the use of double-row fans is practical or not, we will need a basic design, which is a representative of the fan geometry. The simple model of CFM 56-7B-27 turbofan engine fan blade is used in this investigation as a baseline geometry and to check the effectiveness of the proposed system. the fourth state as a basic plan, we need to consider a fixed diameter for the fans, in this respect, the height of the blade and the nose of the fan are equal in all four states and 798 mm and 240 mm are considered respectively.

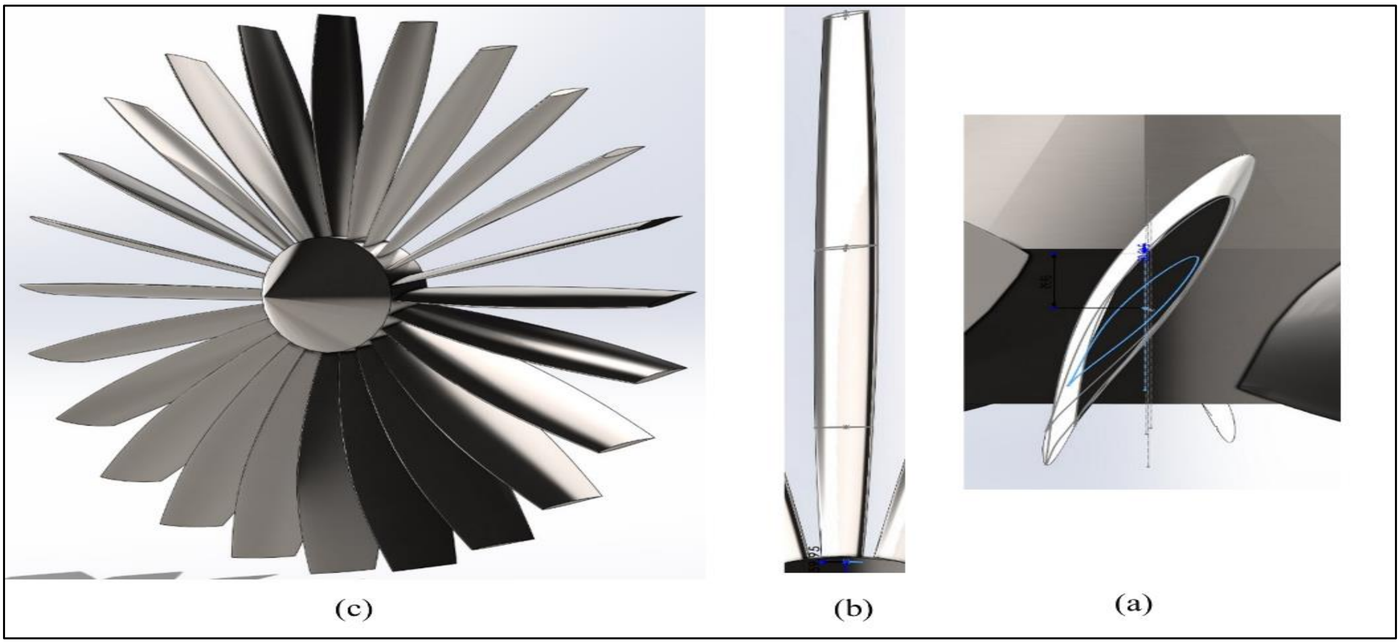

Fig 5 The view of the Sections used in the Geometry of the Basic Design (a and b) and the Final State of the Geometry of the Fourth Design

Of course, it is worth mentioning that the geometry related to the basic design was drawn and simulated in a special way due to the unavailability of the design details of the fan blades of this engine, so that only the results of the fan parameters were consistent with the output data of the CFM 56-7B-27 engine. On the other hand, it should be mentioned that in order to consider the conditions of geometries in the first to third state as the same as

The airfoils used in this fan are NACA airfoils with the numbers EL 210-65 and 410-65, which are set in four sections with different chord lengths in order to have the closest match with the data of the CFM motor fan, although the existence of the basic design as well As its name suggests, it is only as a base, whose data is already known, but in order to make the measurement of this base plan more complete, it was designed and drawn in a way so that its contours are available.

II. ANALYTICAL RESEARCH METHOD OR MODELING

The aerodynamic performance of the fan blade can be described using models and mathematical formulas. One of the commonly used methods is the blade element motion theory. This method decomposes each blade into small elements and analyzes the forces acting on each element. The lift and drag forces on an infinitesimally small blade element can be calculated using the following relations:

$$L = \frac{1}{2} C_L \rho V^2$$

$$D = \frac{1}{2} C_D \rho V^2 dr$$

The orifice affects the Reynolds number, which is a dimensionless parameter related to the flow regime, and affects the lift and drag coefficients. Therefore, the blade opening must be carefully selected to ensure efficient performance over the entire range of operating conditions. Navier-Stokes equations are partial differential equations that describe the motion of viscous fluids. These equations are obtained from combining the laws of conservation of mass, momentum and energy for a compressible or incompressible fluid. For the numerical solution and simulation of turbofan engine fan blades, Navier -Stokes equations are written as follows:

- *Conservation of mass Equation:*

$$\frac{\partial \rho}{\partial t} + \nabla \cdot (\rho \mathrm{u}) = 0$$

- *Momentum Conservation Equation:*

$$\frac{\partial (\rho \mathrm{u})}{\partial t} + \nabla \cdot (\rho \mathrm{uu}) = -\nabla p + \nabla \cdot (\mu \nabla \mathrm{u}) + \rho \mathrm{g} + \mathrm{f}$$

- *Energy Conservation Equation:*

$$\frac{\partial (\rho e)}{\partial t} + \nabla \cdot (\rho e \mathrm{u}) = -p\nabla \cdot \mathrm{u} + \nabla \cdot (k\nabla T) + \rho q + \Phi$$

To model turbulence in fluid flow, methods based on Reynolds averaging are usually used. In this method, flow variables are divided into time averages and fluctuations relative to the average. This causes the Navier -Stokes equations to include additional terms called Reynolds stresses. These stresses indicate the effect of turbulence on the mean flow and should be expressed by turbulence models.

One of the common turbulence models in the Reynolds averaging method is the standard Ka-Omega model, which was presented separately by Kolmogorov (1942) and Saffman (1970). This two-equation model is used to calculate two turbulence variables, which are the specific kinetic energy of turbulence (k) and the specific decay rate of turbulence (ω). ω is proportional to the ratio of the decay rate to the kinetic energy of the disturbance ($\omega \propto \varepsilon/k$) and since it has a dimension of [1⁄s], it is also known as the disturbance frequency. In k-ω models, the length, velocity, and time scales are related by the following relations:

$$u \propto \sqrt{k}, l \propto \frac{\sqrt{k}}{\omega}, \tau \propto \frac{1}{\omega}$$

In the standard k-ω model, the turbulent jet and the transfer equation for the kinetic energy of the turbulence, based on the k-ω model presented by Wilcox (1988), are respectively expressed as follows:

$$v_t = C_\mu \frac{k}{\omega}$$

$$v + \sigma^* v_t \frac{\partial \omega}{\partial t} + \overline{u}_j \frac{\partial \omega}{\partial x_j} = \alpha \frac{\omega}{k} - \tau_{ij}' \frac{\partial \overline{u_i}}{\partial x_j} - \beta \omega^2 + \frac{\partial}{\partial x_j}\left[(v + \sigma^* v_t) \frac{\partial \omega}{\partial x_j} \right]$$

To close the standard k-ω model equations, it is necessary to determine the coefficients $C_\mu, \beta^*, \sigma^*, \alpha, \beta$ and σ. The values of the coefficients of this model are summarized in the following table:

Table 3 Values of coefficients required to close the Standard k-ω model Equations

β^*	β	α	σ^*	σ	C_μ
β^*	0.075	0.5556	0.5	0.5	**1**

The Helm-Holtz equation is a partial differential equation used in physics and acoustic engineering. This equation is used to describe the phenomena of sound and acoustic waves in three-dimensional spaces, so that it allows the calculation of acoustic pressure in different spaces. The Helm-Holtz equation is as follows:

$$\nabla^2 P + (k^2) P = 0$$

In this equation, k is a positive number called the wave number, which depends on the acoustic frequency and the properties of the environment. The solution of this equation for acoustic pressure is done in the form of wave functions with different frequencies and shapes. One of the common ways to solve this equation is to use the method of separating variables. With this method, we divide the acoustic pressure variables as the product of functions of spatial and temporal variables and then insert these functions into the equation and lead to a set of separate equations for spatial and temporal functions. The Helmholtz equation based on the speed of sound can be rewritten as follows:

$$\nabla^2 P - \left(\frac{1}{c^2}\right) \frac{\partial^2 P}{\partial t^2} = 0$$

This equation is obtained based on conservation of energy and equation of motion in fluid mechanics and acoustics. By using some physical relationships related to acoustics and fluid flow, it will be possible to analyze and investigate the changes in sound pressure due to the presence of vanes. One of the important relations that is usually used in this field is the Yukowski-Plan relation. This relationship states that the change in sound pressure relative to atmospheric pressure is proportional to values such as mass density (ρ_0), sound speed in the environment (c), blade speed (U) and the angle between the flow direction and the blade axis or the collision or attack angle (θ). The Yukowski-Plane equation is a mathematical equation used to model the change

ISSN No:-2456-2165 https://doi.org/10.38124/ijisrt/IJISRT24SEP1537

in sound pressure (P) relative to atmospheric pressure (P_0) due to the presence of a solid vane in a fluid flow. This relationship is based on assumptions about fluid flow properties and vane behavior. The Yukowski-Plan relation is as follows:

$$P' = P \times exp\,(ik_0x)$$

In this regard, the Mach number is related to the fluid flow, which shows the ratio of the speed of the blade to the speed of sound in the environment. i in this equation represents a coordinate unit for the solid blade, which is defined as the width of the blade, and the length of the blade is equated with b. The Yukowski-Plan relation is very efficient in modeling sound pressure changes caused by the presence of a solid vane in a fluid flow, and this relationship is usually used in the field of vane acoustics and investigating their effect on sound intensity and air fleets. By combining the Helmholtz equation and the Yukowski-Plan relationship, it is possible to investigate the change in sound pressure due to the presence of vanes.

As a result, the final relation of the Helmholtz equation will be obtained:

$$P'(r,t) = \rho_0 c\,(1 - \frac{c}{U}\cos\theta)$$

Bazian-Siemens equation is one of the important equations in the field of design and analysis of fans and turbines. This equation is developed based on the principles of mass conservation and the saturation equation for air flow in a constant environment. The Bazian-Siemens equation is as follows:

$$v = v_0 \cos\beta\,\sqrt{1 - \frac{c_t}{2}}$$

The Bazian-Siemens equation is developed based on the mass conservation principle for the fan blade system and the saturation principle for air flow in a constant environment. Using this equation, it is possible to check the performance optimization of fan blades and turbines and determine the best blade pitch angle for maximum efficiency.

In the field of aerospace engineering, there are relationships for changes and dependence of the speed and pressure of the outlet air of the fan blades with the changes of the pitch angle of the blades. One of the most famous relations in this field is Bernoulli's relation. This relationship is expressed as follows:

$$P + \frac{1}{2}\rho v^2 + \rho g h = \text{Constant}$$

This equation forms the basis of fluid mechanics and is used in cases such as airplane airfoil design, velocity measurement in channels, and fluid flow analysis, which shows the inverse relationship between velocity and pressure. After designing the geometry of the fan blades and nose in the SolidWorks software environment, the final designs were completed in the Design Modeler software from the Ansys collection. Since the geometry is designed and simulated in real dimensions, as a result, to study the numerical solution in ANSYS Fluent software, the method of movement of grids is used instead of dynamic gridding, so that almost similar results can be achieved in a shorter period of time, so that the cylindrical area that encloses the fan is considered as the rotating area and a larger cylindrical area called the enclosure that surrounds the fan area.

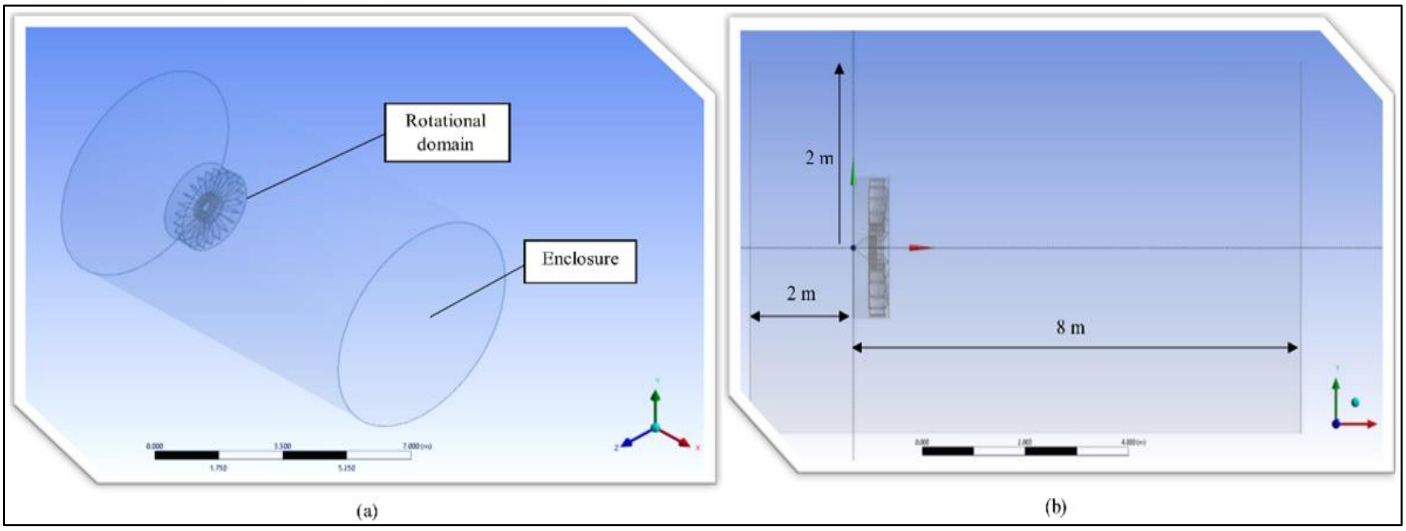

Fig 6 Introducing the Rotating Area and the Built-in Area in the Pre-simulation Stage in Part (a) and the Details of the Area Geometry in Part (b)

The geometry of the rotating area is designed so that it is only 3.5 mm away from the tips of the fan blades. Also, its height is such that it covers the tip and back of the fan and its nose well. A larger cylindrical area is also considered in order to cover the geometry of the problem well. According to the dimensions of the problem, which is in accordance with the reality, the volume of the simulated environmental area will contain about 125,664 cubic meters. An enclosure designing geometry properties to simulate the fan is shown in figure 7. The meshing of the geometries was done automatically in the

ISSN No:-2456-2165 https://doi.org/10.38124/ijisrt/IJISRT24SEP1537

first step in the Ansys meshing software, and then we achieved the appropriate quality by changing the size of each component. The quality of grids was also evaluated with three factors measuring the quality of the skewed grid, aspect ratio and vertical quality, and the best performance in the appropriate grid was selected as the result. In order to be aware of the accuracy of the information obtained from the simulation, each geometry was analyzed and simulated with at least 6 different grid models with the number of grids and the size of the grids to finally end up with a fixed solution.

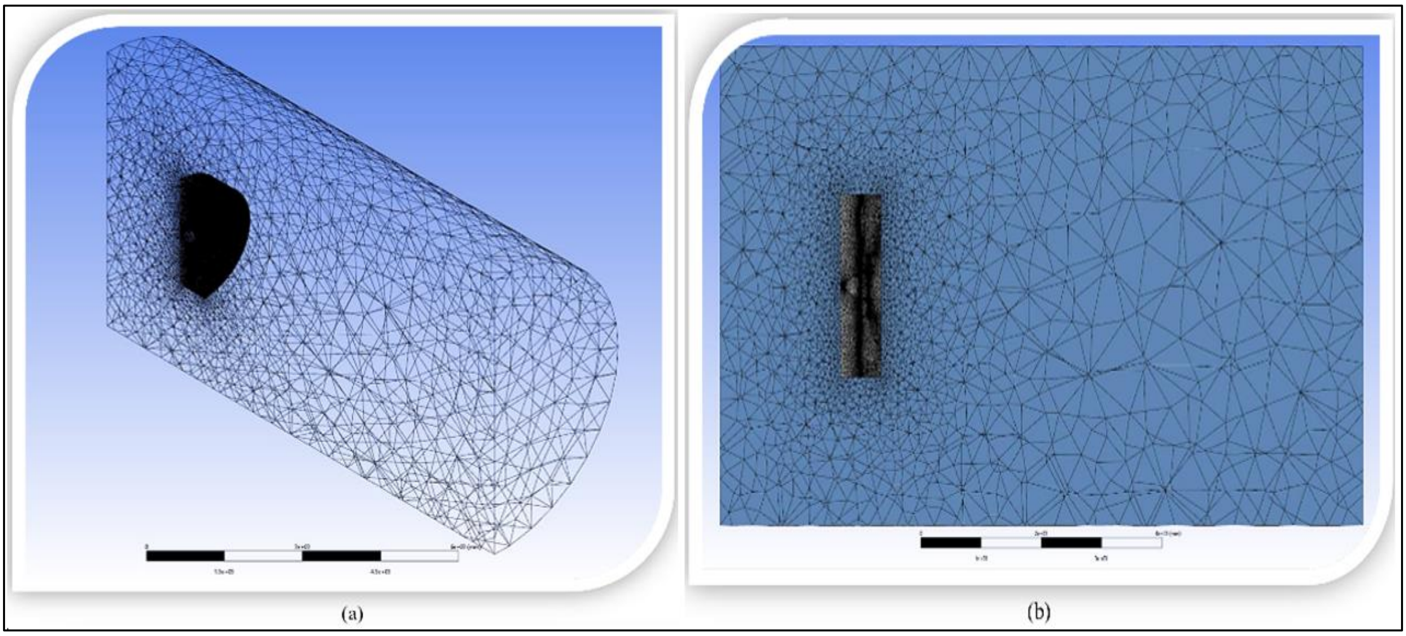

Fig 7 Gridding of the Geometry of the Proposed Design with a Pitch Angle of +12.5 Degrees

More complete information and grid details of all designs are summarized in Table 4, and an example of the grid related to the geometry at a pitch angle of +60.5 degrees is depicted in Figure 8.

Table 4 Meshing Properties in Both Geometry

Geometry Type	Blade Angle	Number of Grids	Grid Size	Skewness			Aspect Ratio			Orthogonal Quality		
				Min	Avg	Max	Min	Avg	Max	Min	Avg	Max
Proposed Geometry	+60.5	1.721648	650	2.6161e-4	0.23577	0.84	1.161	1.84	8.97	0.1505	0.763	0.86
	0	1.948491	588	5.1961 e-5	0.24952	0.88	1.162	1.88	9.96	0.097	0.749	0.82
Reference	-	913665	580	8.4487 e-6	0.2382	0.84	1. 158	1.84	10.46	0.1521	0.7608	0.83

This study aims to present, analyze, and implement a comprehensive design for enhancing the braking efficiency of turbofan engines. This includes the implementation of a variable pitch mechanism, which has been widely adopted in propeller engines over the past few decades. For this purpose, parameters such as pressure, velocity, sound, thrust, and reverse thrust are investigated and analyzed.

To assess the effectiveness of this mechanism, the results of the proposed designs are compared with the results and output data of the conventional fan blade geometry of a typical engine (CFM56-7B-27). The same input parameters are used for the proposed fans to ensure consistent data comparison.

➢ *Validation*

This study utilizes a tandem fan configuration with an inner and outer fan. By adjusting the pitch angle of the outer fan blades, a reverse thrust force is generated. This force can be employed during aircraft landing as an auxiliary braking force to overcome inertia and reduce the acceleration of large aircraft like the Boeing 777, in conjunction with conventional mechanical braking systems. Additionally, due to the use of shorter blades, these tandem fan systems are expected to generate less noise compared to the conventional model. To validate and verify the accuracy of the comparison, three critical parameters of the baseline design have been compared with the data for the CFM 56-7B27 engine available in the engine's technical manual. These comparisons are presented in table 5. [22]

ISSN No:-2456-2165 https://doi.org/10.38124/ijisrt/IJISRT24SEP1537

Table 5 Validation of base Geometry with an actual CFM56-7b 27 Fan Blade Characteristics

Para. \ Geom.	Base Geometry	CFM 56-7B 27 Fan Blade	Error
Thrust [kN]	95.481	97.148	1.7 %
Pressure Ratio	1.79	1.7	5 %
Blade Tip Speed [m/s]	439.213	427	2.8 %

The results obtained from the proposed designs are compared with each other and with the data obtained from the conventional fan blade geometry of the CFM56-7B-27 engine as a baseline design to evaluate the effectiveness of the results. Furthermore, since the input data for the geometry of the base design is available in the engine's technical manual, the results obtained from the simulation of the fourth geometry are compared with the existing output data in the engine's manuals to ensure the accuracy of the output results.

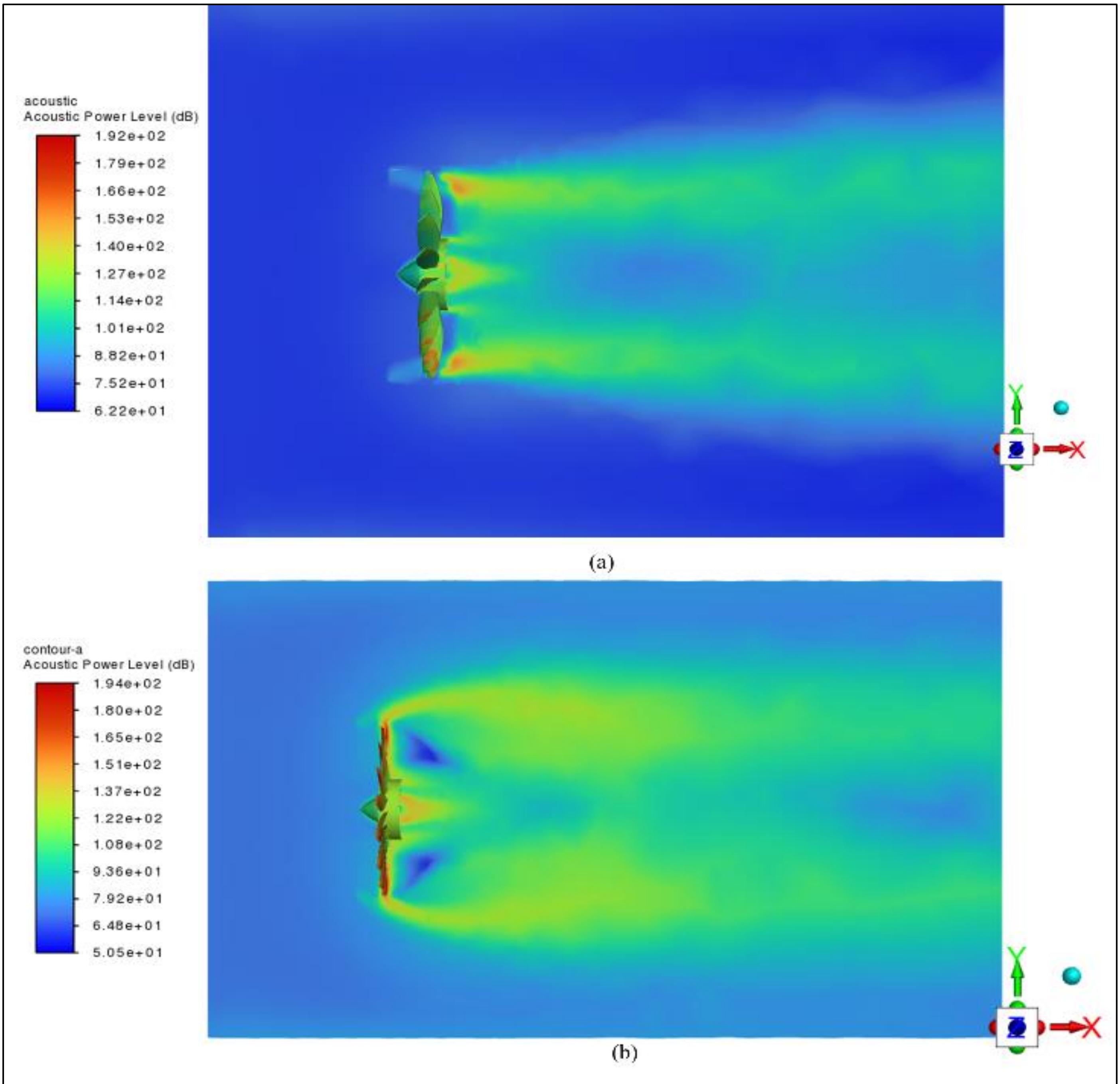

Fig 8 Side view of Sound Intensity Contours for the Second Design Geometry at Two Angles: Zero Degrees and 60.5+ Degrees

ISSN No:-2456-2165 https://doi.org/10.38124/ijisrt/IJISRT24SEP1537

Figure 9 depicts the sound intensity around the rotating fan blades at maximum RPM for generating maximum thrust, with the initial conditions mentioned earlier. The air enters the engine at the maximum allowable speed for the CFM56-7B engine. In this case, as shown in image (a), the sound field generated upstream of the blades is limited to the trailing edge of the tip of the second-row blades and the hub region. The average sound intensity values for these regions are 158 and 146 decibels, respectively. The sound intensity in the wake generated upstream of the blades is 116 decibels on average, decreasing to 105 decibels as the distance from the blades increases. With a further increase in the pitch angle, which is implemented to generate reverse thrust, it is observed that the sound-affected area expands compared to the previous case. The sound intensity of the exhaust gases from the fan blades reaches 125 decibels, extending up to 6 meters downstream, unlike the previous case where the sound intensity of the gases in the hub and first-row fan only extended up to 1 meter. However, the sound intensity decreases from 106 to 97 decibels between 3.5 and 6 meters from the blades. Additionally, Figures 10 and 11, which show the sound intensity contours in the front view and on the fan blades, respectively, indicate that the second-row fan blades will operate in a region where the sound intensity is highly unpleasant for the human ear. The blades will operate in an area with an average sound intensity of 163 decibels for approximately 80% of their length from the tip. This value increases to 186 decibels at the tip of the blades. Images (a) of Figures 9 and 10 also show the sound intensity contour distribution at zero angle of attack, where the blades operate under ideal conditions. Only a small portion of the blade tip will have a sound intensity of 151 decibels.

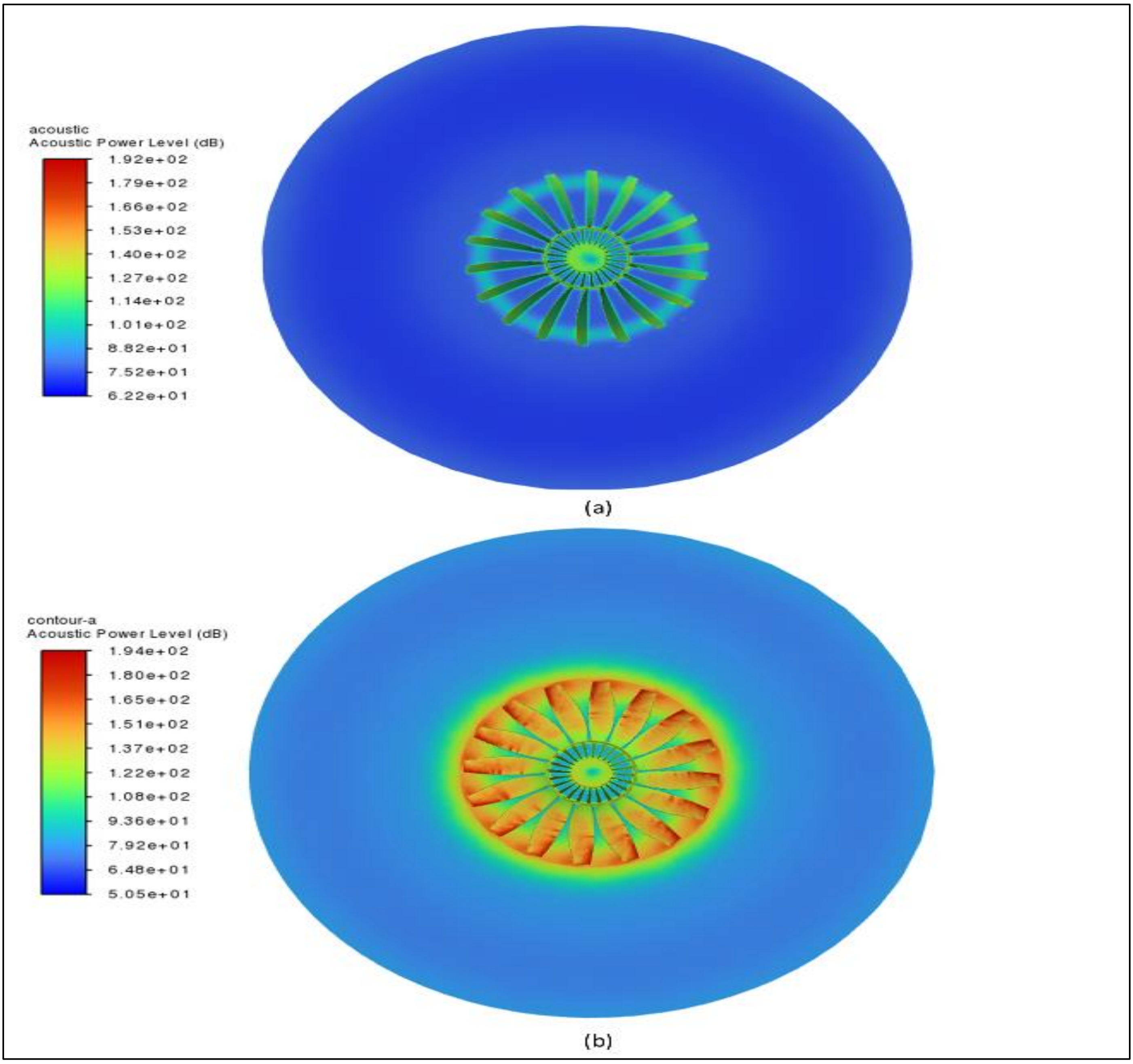

Fig 9 Front view of Sound Intensity Contours for the Second Design Geometry at Angles of Zero Degrees and 60.5+ Degrees

ISSN No:-2456-2165 https://doi.org/10.38124/ijisrt/IJISRT24SEP1537

The velocity distribution contours for the second design geometry, shown in Figures 10 and 11, indicate that in the first case, where the blade pitch angle is 12.5 degrees and the inlet air has a speed of 660 km/h, the air velocity near the fan blades reaches 1355 km/h. After passing through the blades, the air velocity increases to a maximum of 1796.35 km/h. Then, as the air moves upstream of the blades, it gradually reaches 1256.4 km/h at approximately five meters from the blades. However, a high-velocity region extends up to 2.5 meters after the blades, with an approximate velocity of 1519 km/h at the outlet. The high-velocity region contains vortices and turbulence, whose locations are marked in Figure 4-14. The highest velocity in this pitch angle, as expected, occurs at the tip of the second-row fan blades, reaching 2214 km/h. With an increase in the pitch angle of the second-row fan blades by 60.5 degrees, it is observed that the high-velocity region upstream and downstream of the blades disappears to some extent. The velocity of the exhaust air after approaching and passing through the second-row fan blades decreases significantly. In the downstream region, the air has a maximum velocity of 158.4 km/h and a minimum velocity of 120.24 km/h, which occurs near the second-row fan blades. This velocity decreases to 38 km/h at a distance of 50 centimeters from the blades, except for a very thin layer of high-velocity air formed at the trailing edge of the blades, which has an approximate velocity of 1969.2 km/h. However, it is worth noting that in this case, the exhaust air from the second-row blades at the base of the blade has a higher velocity than the exhaust air from the middle and tip of the blade. This is due to the twist angle in the blades, which increases the pitch angle at the tip of the blades, resulting in a higher velocity reduction. The velocity of the exhaust air from the base of the second-row fan blades increases to 774 km/h.

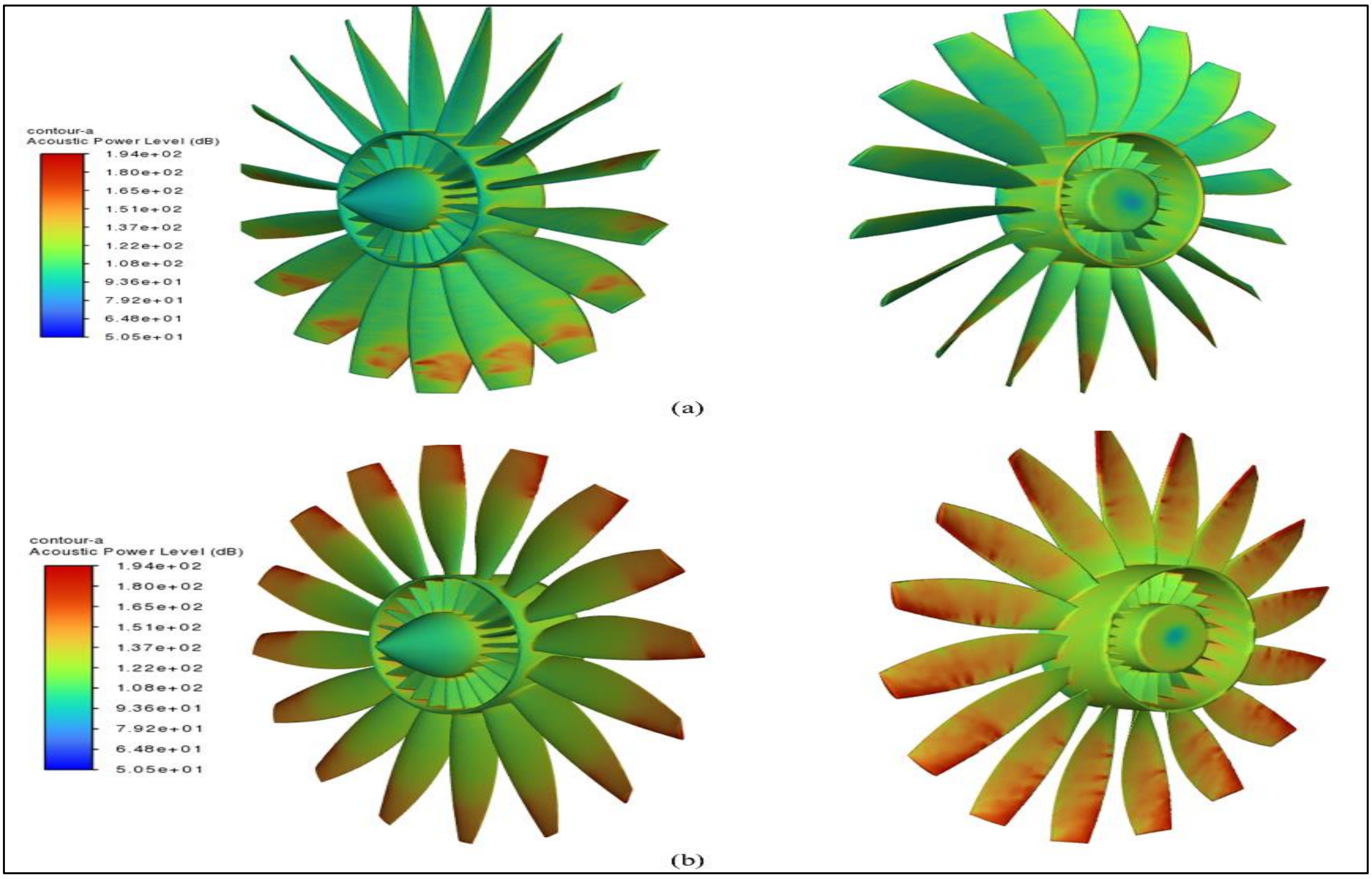

Fig 10 Sound Intensity Contours on the Fan Blades of the Second Design Geometry at Angles of Zero Degrees and 60.5+ Degrees

It should also be mentioned that in this case, the velocity of the exhaust air from the first-row fan blades is around 1386 km/h, which is responsible for feeding the engine and rotating the compressor and other engine components. It is also observed that the average velocity of the exhaust air from the fan blades when generating reverse thrust reaches approximately 62.5 meters per second upstream of the blades. This represents a 108% improvement in the maximum velocity value in reverse thrust mode compared to the results obtained in Reference 29. In the static case, the velocity also increases to 83.6 meters per second, which shows a 54% improvement.

As previously discussed in relation to the velocity contours and the impact of changing the blade pitch angle on the air velocity values passing through the second design geometry fans, increasing the pitch angle also leads to a decrease in the air velocity exiting the fans with variable pitch angle capability, whether these changes are made in the positive or negative direction. In this context, a section of the mid-blade is considered in Figure 12 to show the changes in air velocity passing through the fan blades. From the contours drawn, it can be concluded that the air passing through while the pitch angle is zero degrees has a high velocity passing through the fan blades, such that this velocity has a maximum of 2203 km/h, which corresponds to the tip areas of the second-row fan blades, and the rest of the air will exit the blades at an average velocity of 1476 km/h. In addition, it has been observed that the air around the fan passes at a lower velocity (approximately 602 km/h) compared to the air velocity entering from around the fan. Part (b) shows the velocity contour when the pitch angle is increased by 60.5 degrees, where the air loses its velocity between the blades and except for the leading and trailing edges of the blade where the air moves at an average velocity of 1202 km/h, the air velocity in the space between the blades will reach around 619 kilometers. However, with increasing radial distance from the fan blades, this velocity increases from 784.5 to 830 km/h and then gradually decreases until it becomes equal to the air velocity entering. The air between the blades also has a velocity in the range of 453.6 km/h to 745.2 km/h. The minimum of this velocity occurs behind the trailing edge of each blade in the section where the chord length of the airfoil is at its maximum.

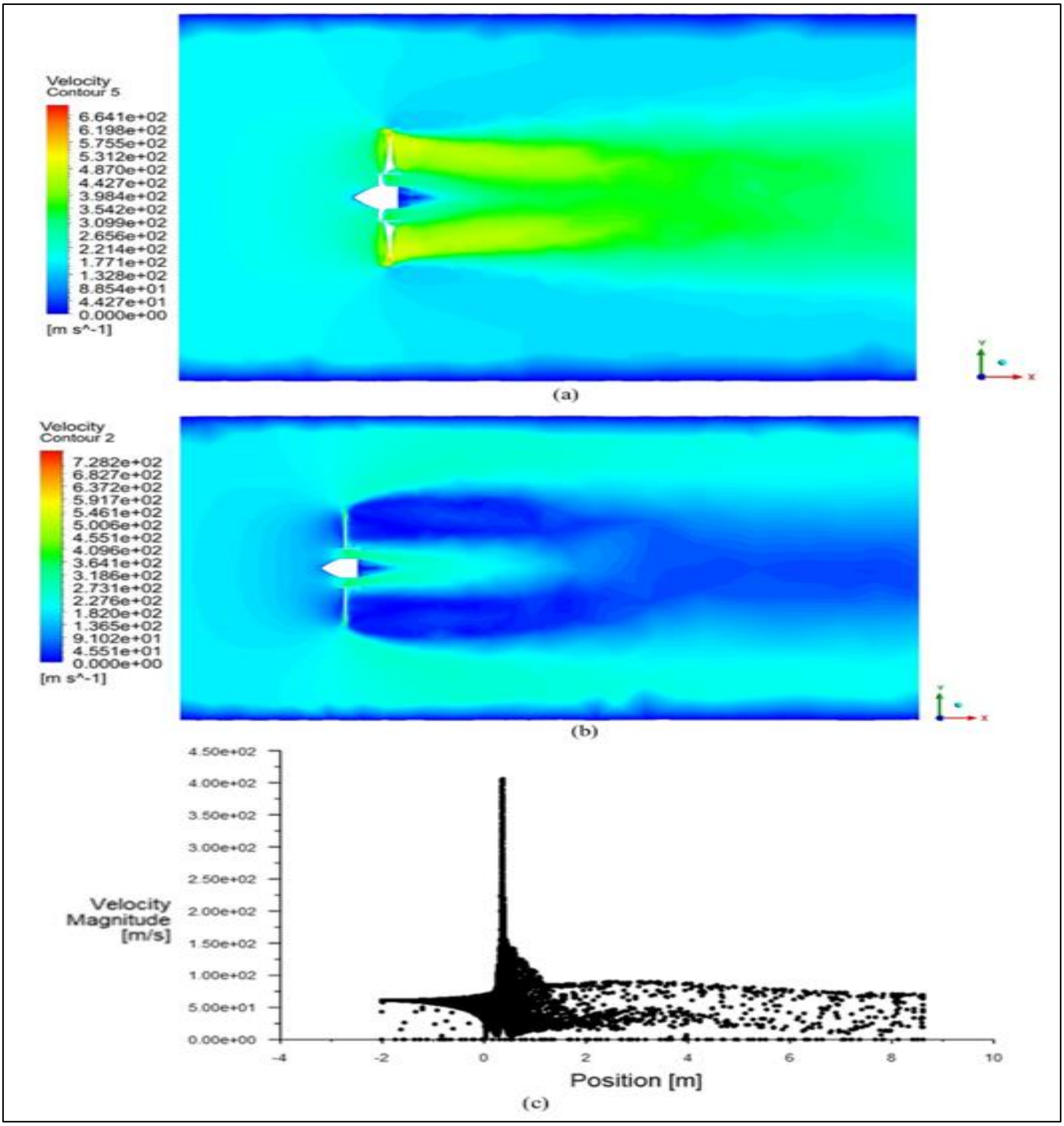

Fig 11 Side view of velocity contours for the second design geometry at two angles: zero degrees and 60.5+ degrees (cases A and B), velocity distrib2ution scatter in the inverse flow state related to the second design geometry (case C)

The velocity distribution on the fan blades is shown in Figure 4-16 for both pitch angles, which indicates a uniform velocity distribution at both angles, indicating that the velocity on the surface of the blades remains unchanged at both blade pitch angles and the velocity changes will only affect the air passing through the blades.

The pressure distribution contours for the second geometry blades at two pitch angles are shown in Figure 4-17, which shows the pressure intensity in the areas around the blades, such that the pressure in the upstream and downstream of the fan blades is much greater than that around it. On the other hand, it is observed that the absolute value of pressure increases as we move towards the tip of the blades, and the reason for this can be explained as follows: as we move towards the tip of the blades and away from the center of the fan, the angular velocity and consequently the total velocity of the blades increase, which according to equation 42-3, this increase in velocity will also lead to a decrease in the pressure value. As expected, the basic design of the fan blades is such that a relatively strong suction creates a large volume of air to pass through the fan blades at a high velocity, which ultimately leads to the creation of thrust. Similarly, the presence of negative pressures in these contours also indicates the occurrence of suction, which is clearly visible in the upstream and downstream of the blades, such that with increasing radial distance from the lateral areas of the blade, the pressure has small positive values, which are less than the ambient pressure under standard conditions.

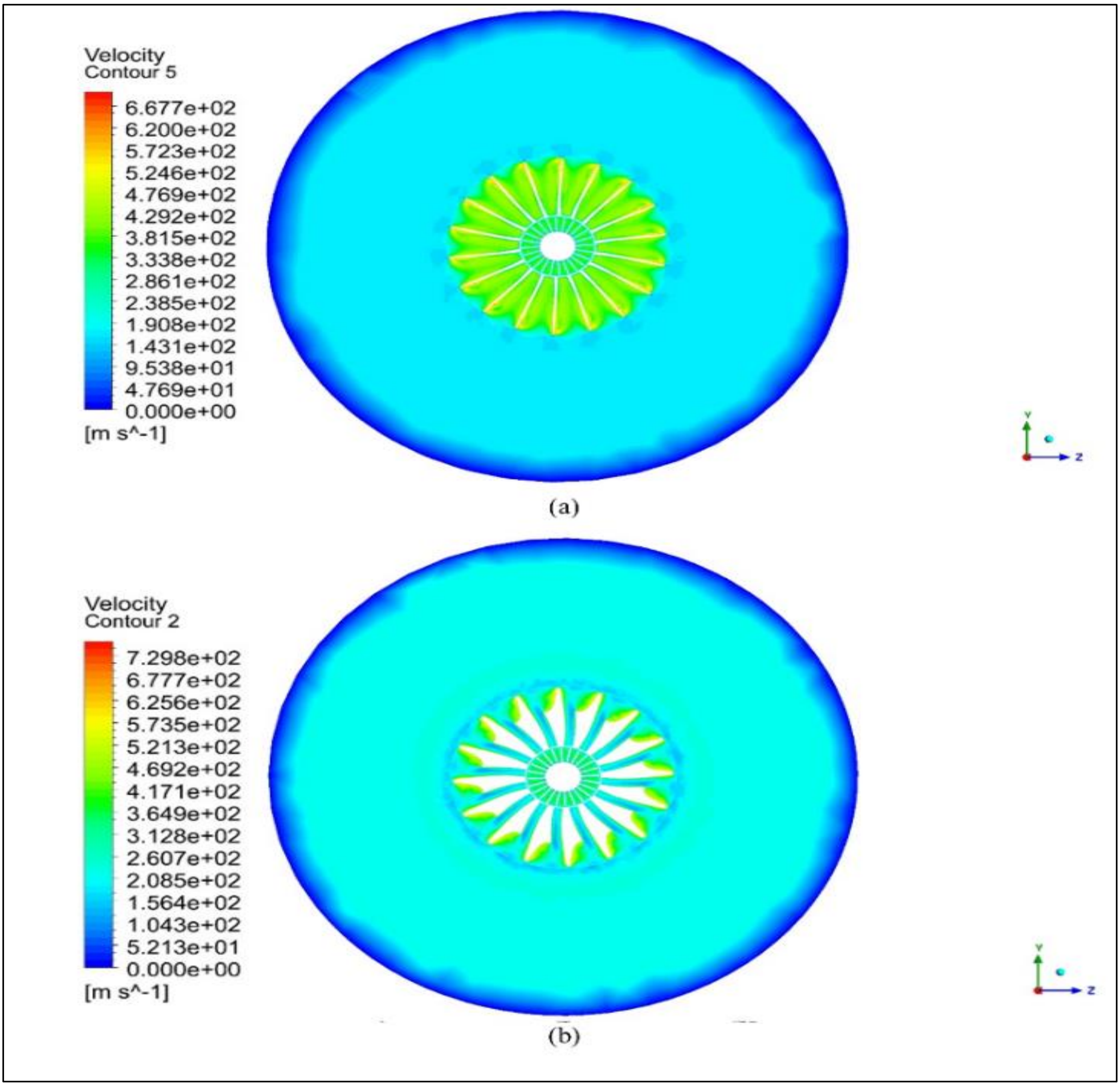

Fig 12 Front view of Velocity Contours for the Second Design Geometry at Angles of Zero Degrees and 60.5+ Degrees

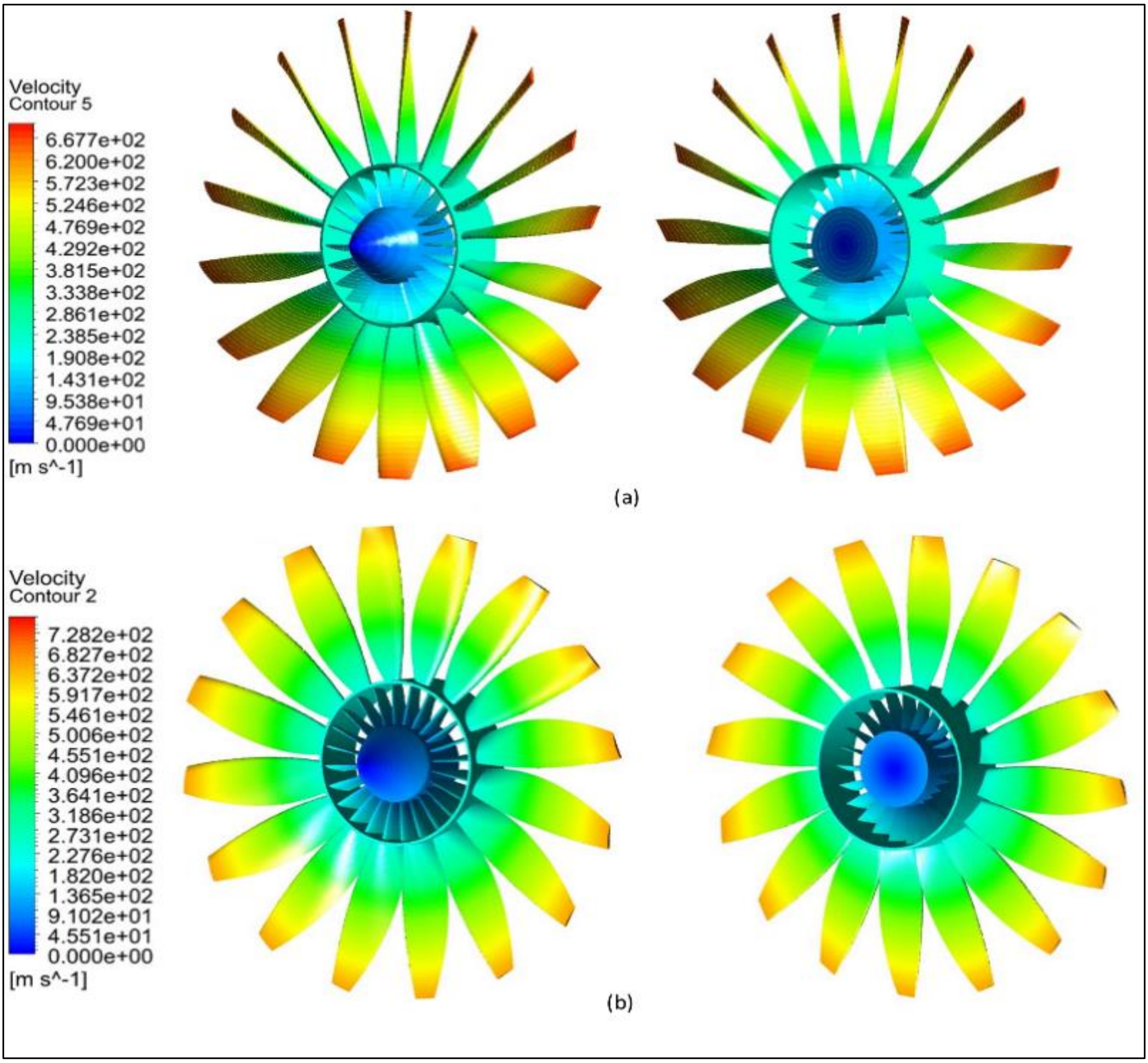

Fig 13 Velocity Contours on the Fan Blades of the Second Design Geometry at Angles of Zero Degrees and 60.5+ Degrees

With an increase in the pitch angle by 60.5 degrees in the direction of rotation of the blades, it is observed that the values and direction of pressures around the blade have changed in such a way that the downstream of the blade has positive pressure values and the downstream of the blade has negative pressures, which means that in this case, a reverse flow against the direction of the incoming flow is being formed, which can be used as a "reverse thrust". It is also observed that when the pitch angle of the blades is increased, the pressure value in the upstream of the blade becomes larger than the pressures in the downstream, which leads to the movement of air from the high-pressure area to the areas with lower pressure. In addition to the above points, it should be mentioned that with the change in the pitch angle of the blade, the upstream areas of the blade are generally affected, such that by using such a concept and geometry in a turbofan engine, it can be expected that the air passing over the engine body after separating from the surface in the case where the pitch angle of the blades changes, has the ability to return from the bypass duct outlet to the fan section after cooling the engine center and passing through the fan blades, causing a reverse thrust. Figure 15 also emphasizes the occurrence of reverse thrust when the pitch angle of the blades changes, such that in part (a), where the pitch angle at the base of the blade is zero degrees, the air passing through the lower surface of the fan blades has higher pressures than the upper surface of the blade, which indicates the principle of blade and airfoil design, such that the pressure difference created on the two upper and lower surfaces of the blade will lead to the creation of torque, thrust, lift and drag. With increasing pitch angle, the pressure of the air passing through the blades will have larger positive values, such that the pressure at the leading edge of the blades increases sharply and exerts a pressure of about 140 kilopascals on the fan blades.

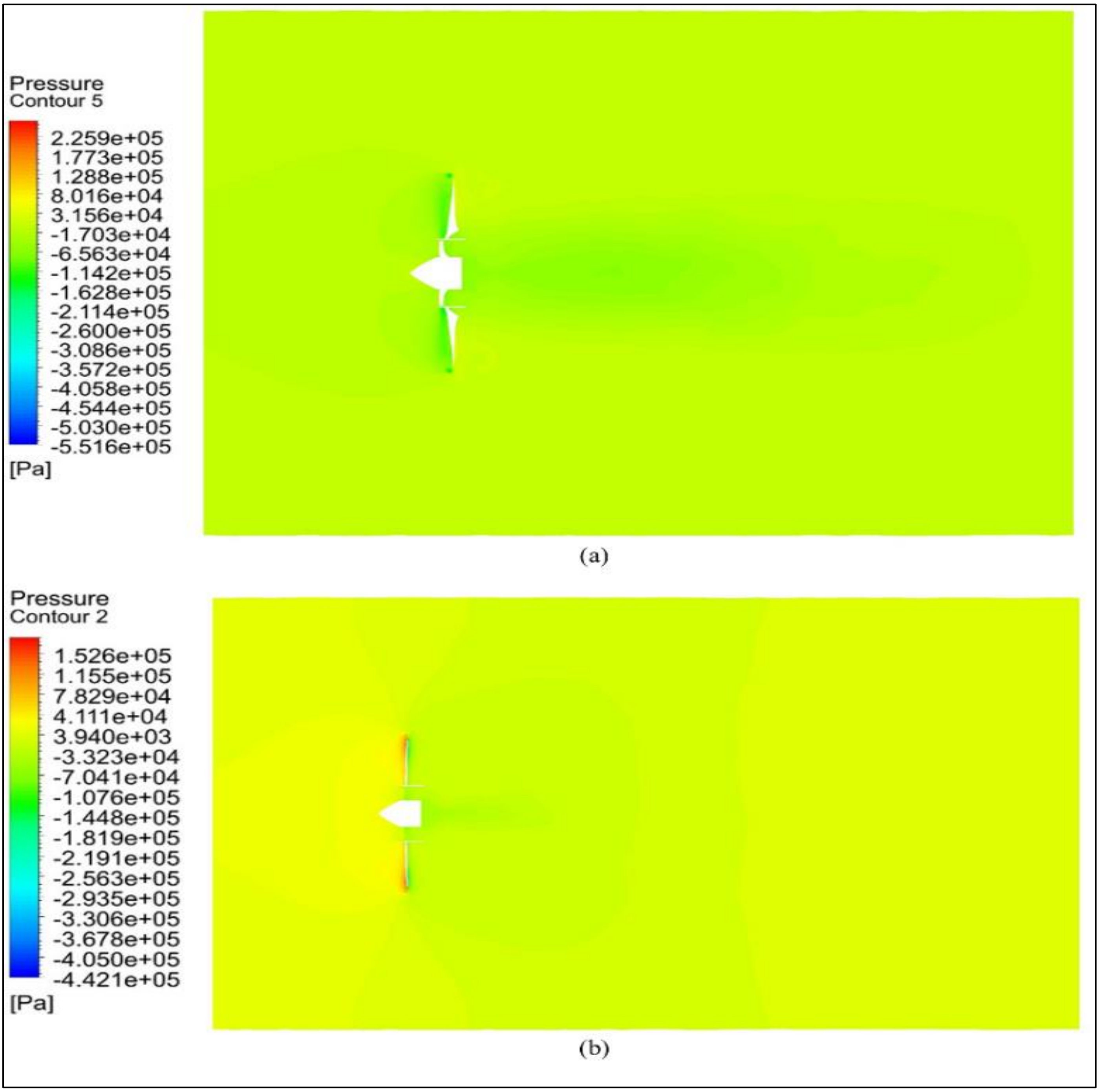

Fig 14 Side view of Pressure Contours for the Second Design Geometry at Angles of Zero Degrees and 60.5 Degrees

Figure 16 shows that when the blade pitch angle is zero degrees, the upper surfaces of the fan blades are responsible for sucking in air. Due to the suction and the increase in the speed of the air passing through the fan blades, the pressure on the lower surfaces of the blades increases and has positive and large values compared to their opposite surfaces. However, with the increase in the blade pitch angle, the opposite phenomenon will occur, and the pressure on the upper surfaces of the blade will increase sharply, but the leading edges of the blade, which are opposite the returning airflow, will have large negative pressure values, which means the occurrence of reverse flow to produce reverse thrust in the fan blades. The thrust generated when the blades have a pitch angle of zero degrees will reach 292.917 kN, which is an increase of about 27 kN compared to the previous geometry. However, with a decrease in the increase in the blade pitch angle to 60.5 degrees, the fan blades with the same input characteristics as the zero-degree input will act as a windmill and generate a reverse thrust of about 181.394 kN. Although the generation of such reverse thrust is natural for a windmill, it should be avoided in the design of fan blades for turbofan engines. Therefore, the air inlet velocity and engine rotational speed are considered with the engine input specifications at the time of aircraft landing, which are 220 km/h and 3200 revolutions per minute, respectively, to obtain a reverse thrust of 25.077 kN. The sound intensity, velocity, and pressure contours are shown in Figures 17, 18, and 19, respectively.

ISSN No:-2456-2165 https://doi.org/10.38124/ijisrt/IJISRT24SEP1537

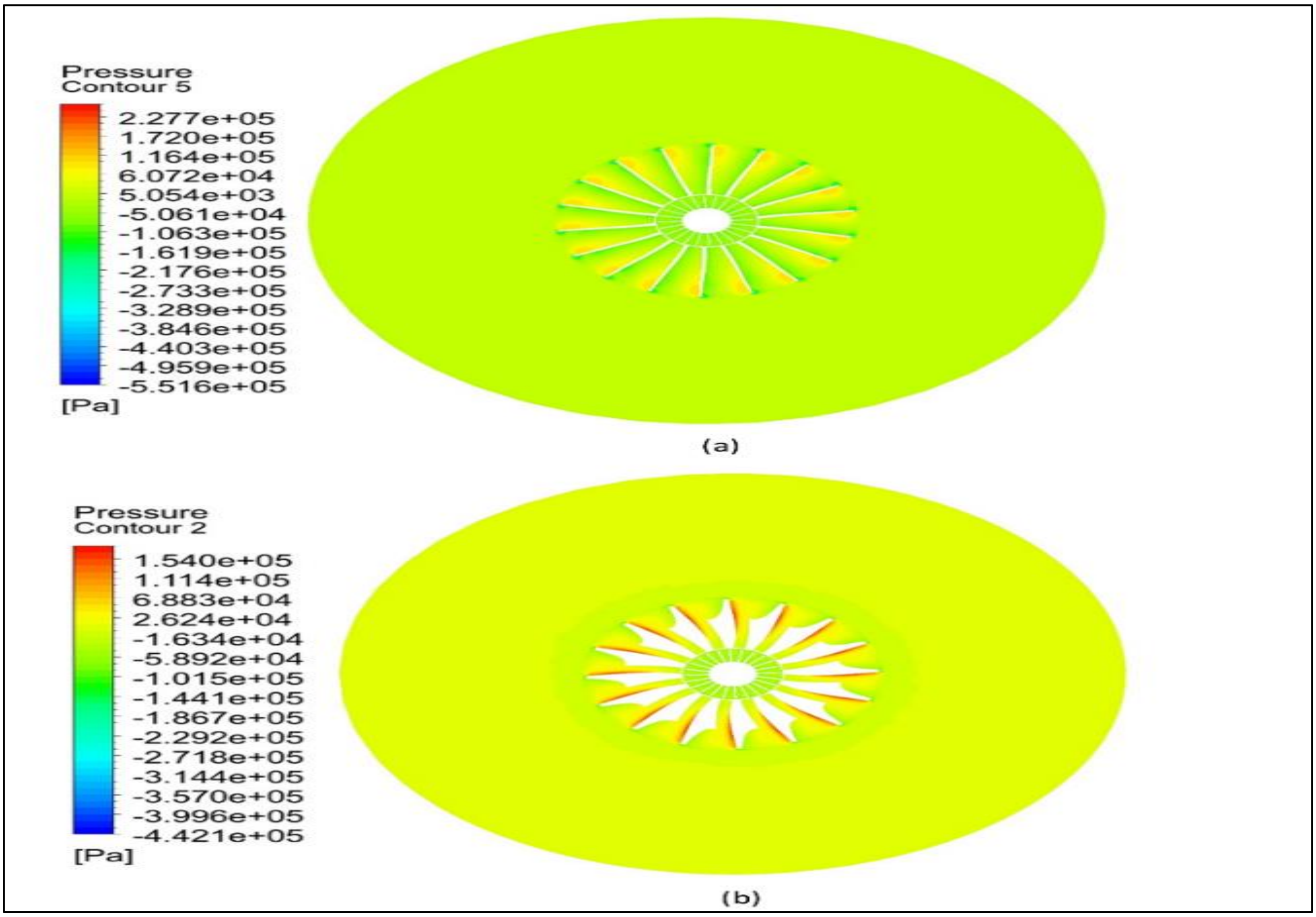

Fig 15 Front view of Pressure Contours for the Second Design Geometry at Angles of Zero Degrees and 60.5 Degrees

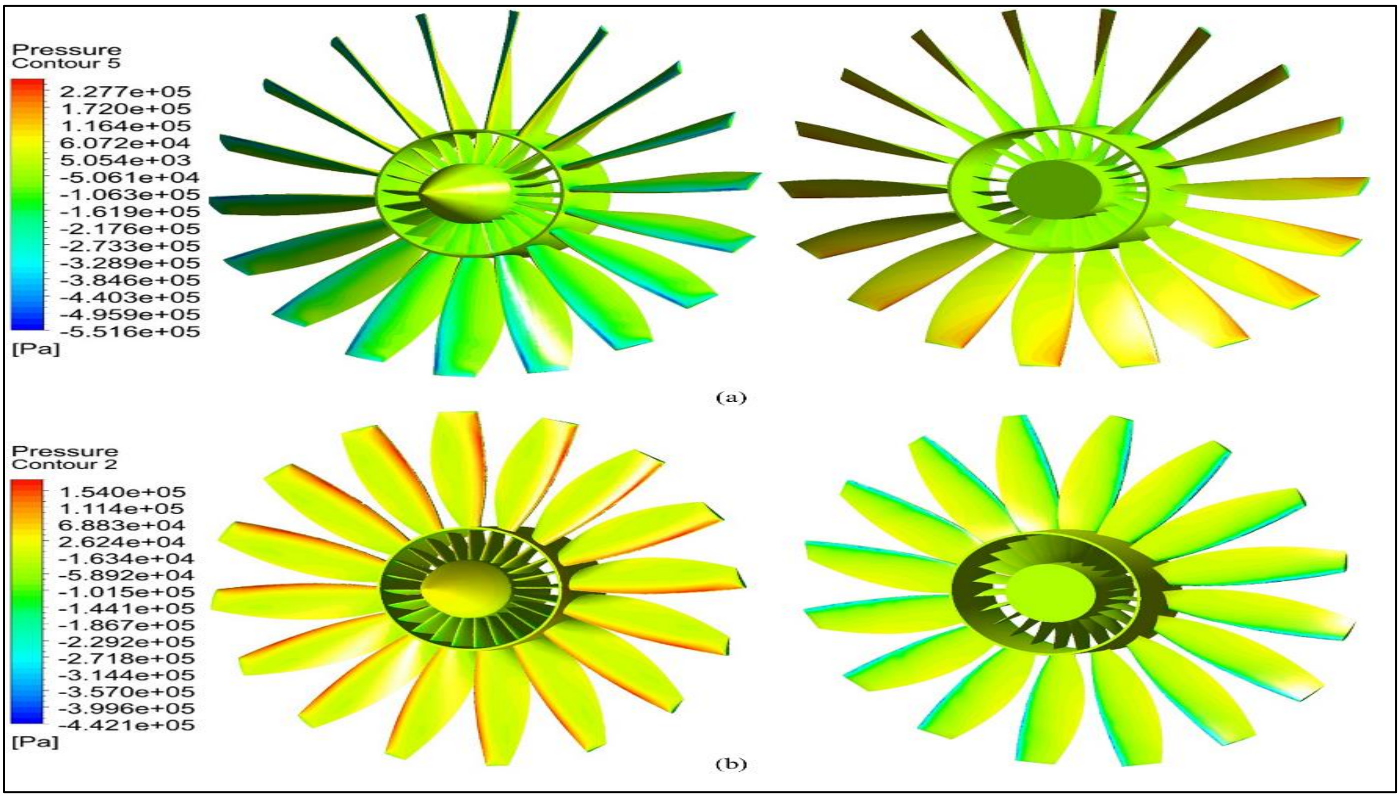

Fig 16 Front view of Pressure Contours for the Second Design Geometry at Angles of Zero Degrees and 60.5 Degrees

ISSN No:-2456-2165 https://doi.org/10.38124/ijisrt/IJISRT24SEP1537

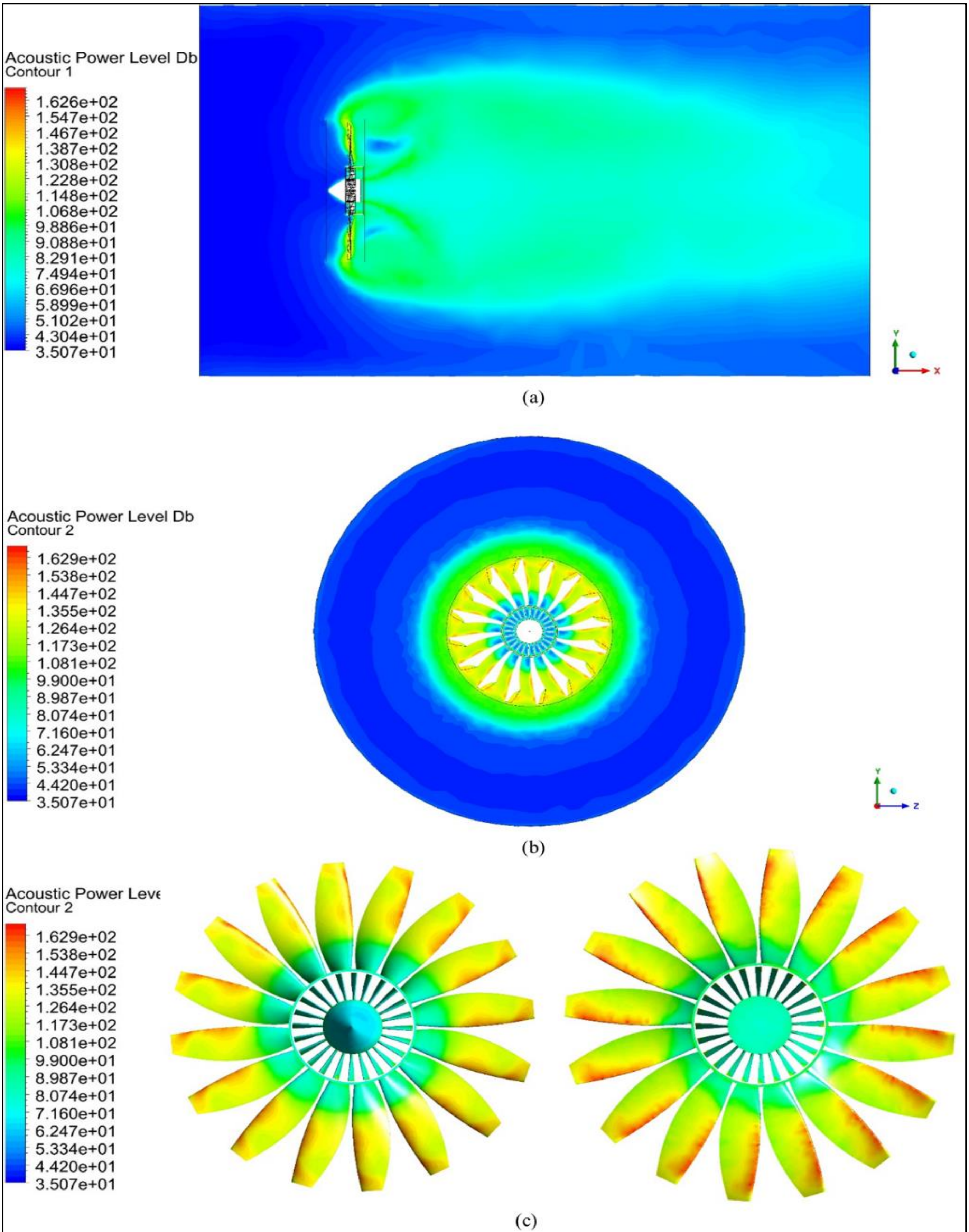

Fig 17 Sound Intensity Contours for the Proposed Design Geometry at a Rotational Speed of 3200 Revolutions Per Minute and an Inlet Velocity of 220 km/h.

ISSN No:-2456-2165 https://doi.org/10.38124/ijisrt/IJISRT24SEP1537

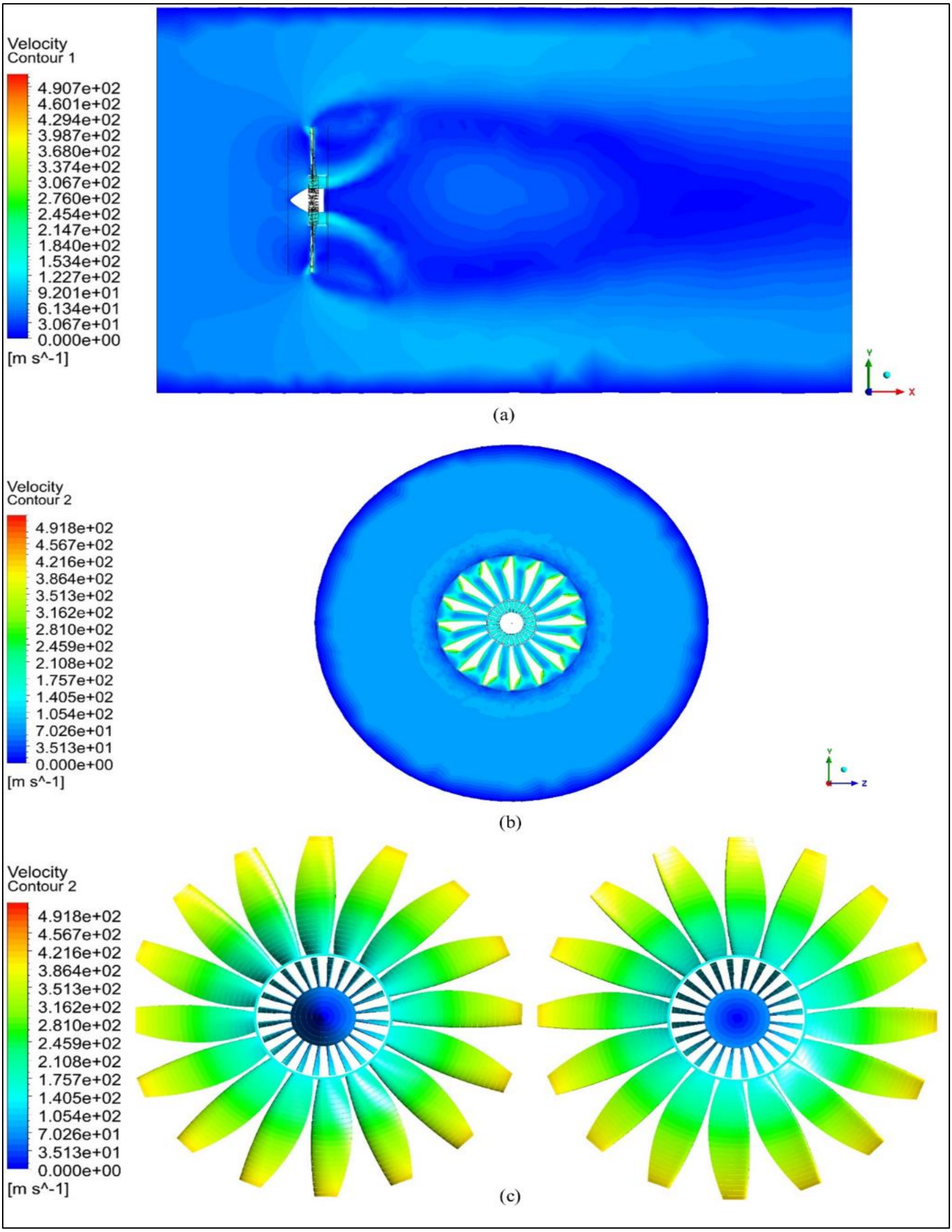

Fig 18 Velocity Distribution Contours for the Proposed Design Geometry at a Rotational Speed of 3200 Revolutions Per Minute and an Inlet Velocity of 220 km/h

The results show that the sound intensity of the air exiting the blade will be in the range of 80 to 135 decibels, with the maximum sound intensity occurring at the surface of the blade. The exit velocity of the air from the first row of blades in this case will change slightly compared to the inlet air velocity, so that the air enters the engine components at a maximum speed of 665 km/h. However, the exit velocity of the air from the second row of blades will be a maximum of 245 kilometers. The data obtained from Figure 20 interprets the pressure contours as follows: except for the back surface of the blade, where the suction will be up to 40 kPa, the pressure in the areas around the blade is also suctioned and decreases up to 10 kPa in some distant points. However, the pressure at the leading edge of the upper surface of the blade and also in the downstream area of the blade takes positive values.

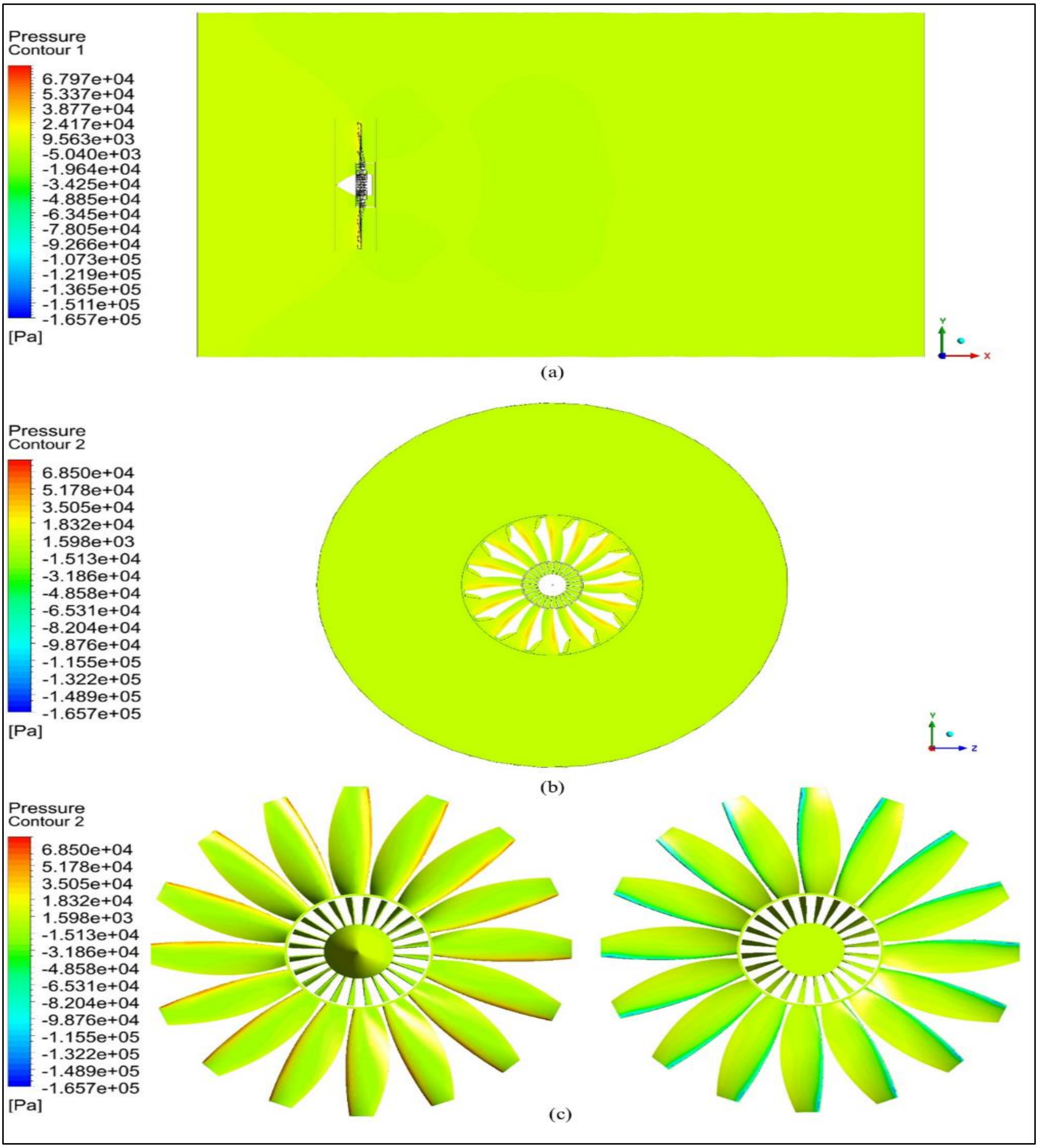

Fig 19 Pressure Distribution Contours for the Proposed Design Geometry at a Rotational Speed of 3200 Revolutions Per Minute and an Inlet Velocity of 220 km/h

ISSN No:-2456-2165 https://doi.org/10.38124/ijisrt/IJISRT24SEP1537

After examining the proposed geometries, in this section, the data related to the fan blades of the CFM56-7B-27 engine will be analyzed and investigated to obtain a suitable reference for measuring the efficiency of the proposed blades. Since the fan of the mentioned turbofan engine only includes one row of fan blades that do not have the ability to change the pitch angle, these blades are simulated only at one angle to use its output as a reference point in comparing the proposed cases.

The data obtained from the simulation of the sound intensity distribution of the fan blades shows that the sound intensity of the inlet air increases slightly as it approaches the fan blades, so that it reaches its maximum value in the upper half of the space between the blades and the trailing edge of the tip of each blade. According to Figure 21-(a), the sound intensity in this area ranges from 138 to 176 decibels, with the maximum value occurring at the largest cross-section of the blade. The sound intensity of this high-speed air will decrease to about 125 decibels at a distance of 3 meters from the blade after passing through the blade. In this geometry, the air around the blade is less affected by the high-speed air passing through the blade, and the average sound intensity of this air is 75 decibels. The air passing through the base of the blades has a sound intensity of 110 decibels, which decreases to 95 decibels as it moves towards the downstream of the blades and behind the engine nose cone. Figures 21-(b) and (c) also emphasize that the maximum sound intensity always occurs at the tip of the blade, although it should be mentioned that in this case, the maximum sound intensity originates from the tip of the lower surface of each blade and decreases as it moves towards the base of the blade, then increases slightly and finally ends at about 121 decibels.

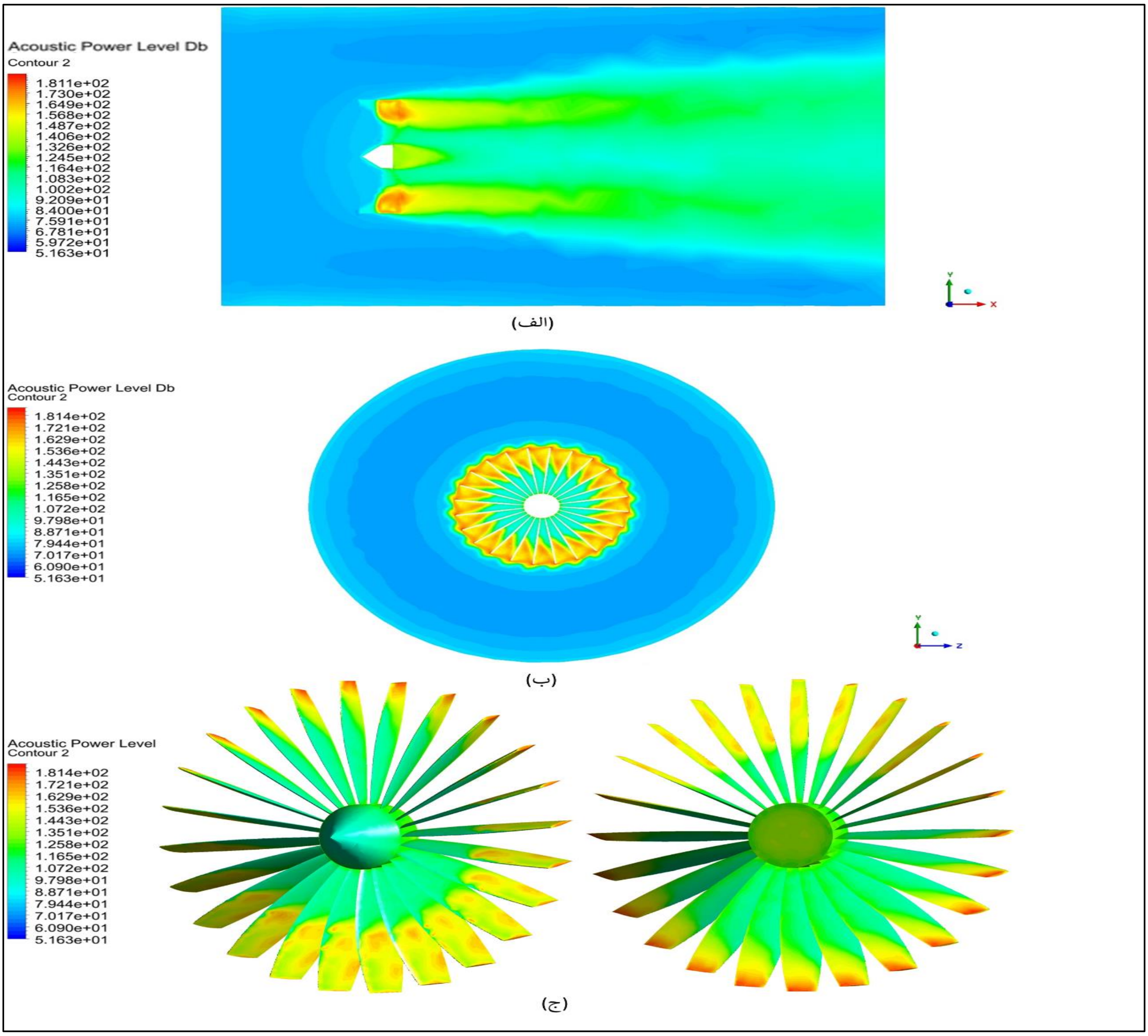

Fig 20 Sound Intensity Variations on the (a) Lateral Section, (b) Midsection Passing through the Blade, and Reference Blade Surface Related to the Fan Blade (c).

ISSN No:-2456-2165 https://doi.org/10.38124/ijisrt/IJISRT24SEP1537

The distribution of velocities for this geometry, shown in Figure 22, shows that the maximum velocity in these blades is about 2455 km/h, which occurs near the tip of the blades, and the rest of the air passing through the blade has an average velocity of 1929.6 km/h, which decreases to 932.4 km/h at the base of the blade where the blade connects to the fan nose cone. The high-speed gas exiting the fan extends up to about three meters from the blade at a speed of 1922 km/h and then gradually begins to decrease, so that at 6 meters from the blade, it will have an approximate speed of 1036 km/h. Behind the fan nose cone, due to the existence of flow vortices, the velocity of the vortex flow is in the range of 99 to 741 km/h. Due to the mutual effects of the fan rotation on the surrounding air, the velocity of the flow passing around the fan initially decreases slightly and then increases as it mixes with the high-speed air exiting the fan, so that the inlet and outlet air velocities are almost equal in front of the blade.

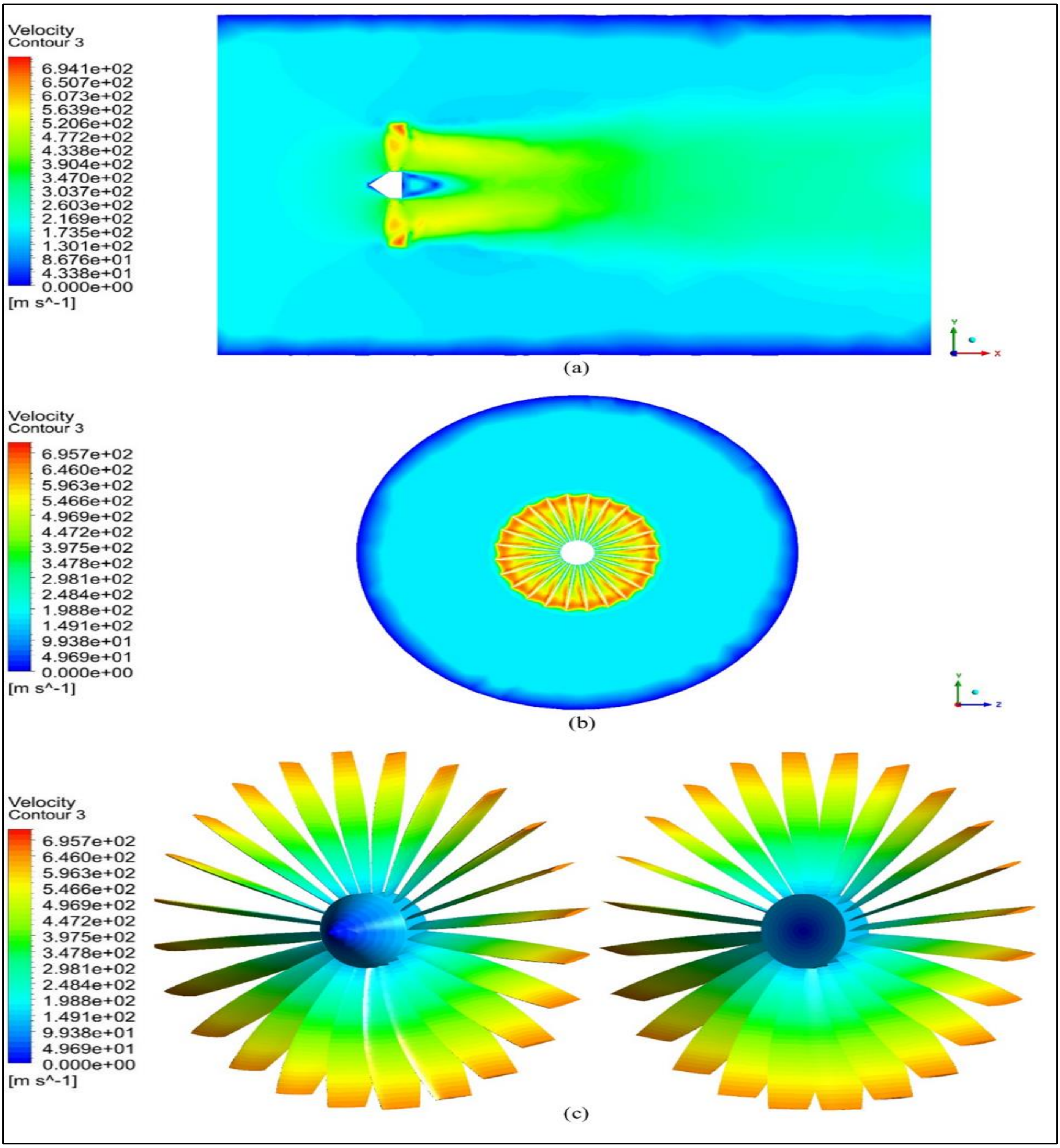

Fig 21 Velocity Variation Contour on the (a) Lateral, and (b) Frontal view, and Reference Blade Surface Related to the Fan Blade (c).

ISSN No:-2456-2165 https://doi.org/10.38124/ijisrt/IJISRT24SEP1537

The pressure distribution contour for the case where only a single row of fan blades without pitch angle change capability is used is shown in Figure 23. These images show that the upstream flows of the swept blade gradually increase in negative pressure as they move towards the blades, reaching a pressure of -63 kPa near the blade. This pressure increase continues into the inter-blade space, reaching -150 kPa, and then drops to approximately -56 kPa just downstream of the blade. Due to the presence of vortex flows behind the fan hub, the air pressure drops to -121 kPa. From the pressure contours, it can be concluded that the pressure decreases as we move from the base of the blades to their tip.

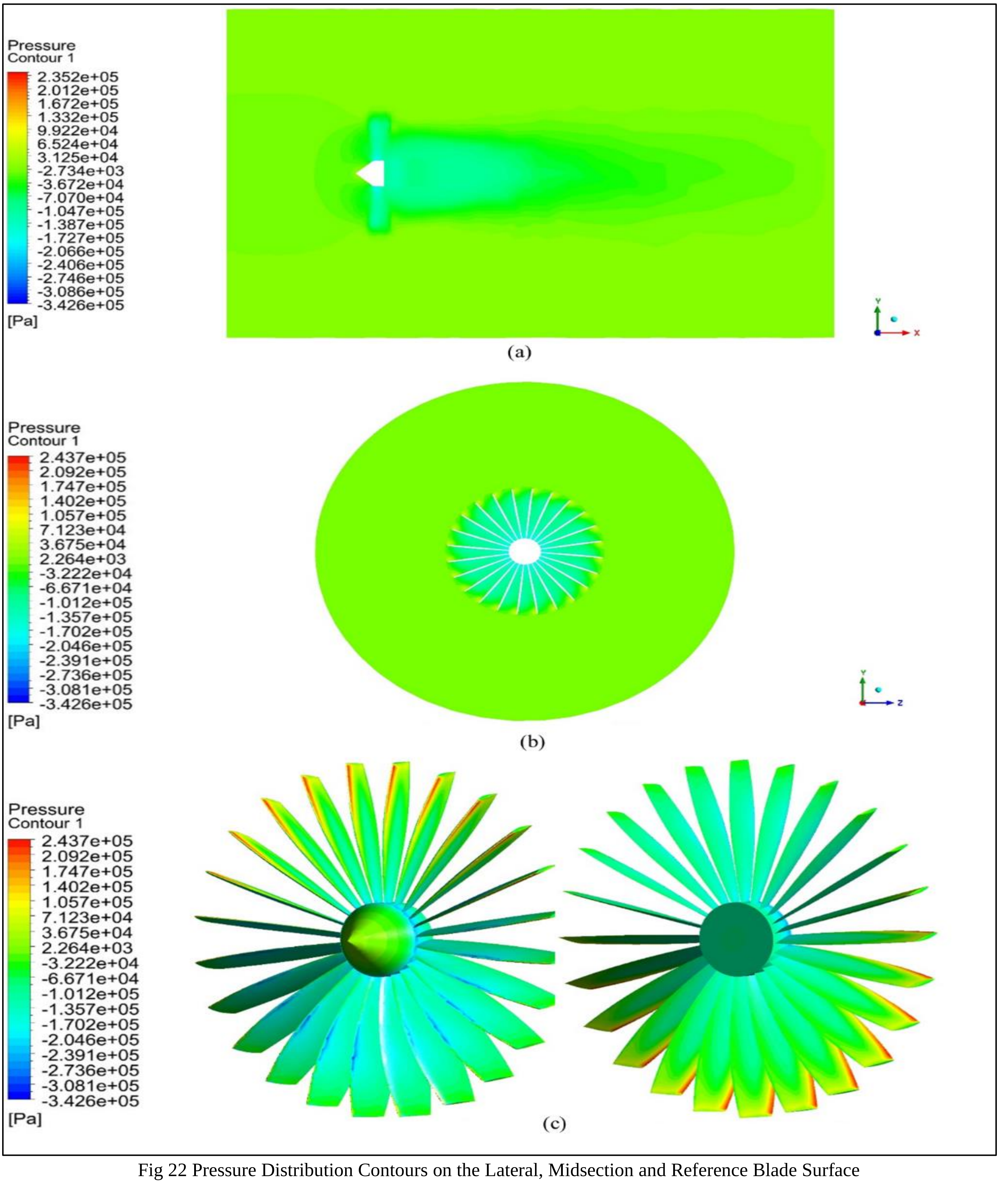

Fig 22 Pressure Distribution Contours on the Lateral, Midsection and Reference Blade Surface

ISSN No:-2456-2165 https://doi.org/10.38124/ijisrt/IJISRT24SEP1537

As observed in the pressure contour of Figure 23-(c) on the blade surface, the lower surface of the blades has large and positive pressure values, while the upper surface of each blade has large negative pressure values. The maximum pressure generated on the lower surface of the blades, which corresponds to the blade tip, is approximately 215 kPa at the leading edge of the blade, and this pressure value decreases to an average of 70 kPa at the blade tip. Meanwhile, the maximum suction pressure, which occurs at the mid-point of the leading edge of the upper surface of the blade, is approximately -290 kPa. The pressure on the fan hub also decreases from +90 kPa at the blade tip to -86 kPa at its end. The thrust produced by this geometry is 95.481 kN, which perfectly matches the thrust of the CFM56-7B-27 engine, which is 121.436 kN.

The simulation results showed that for the second design geometry, which is based on the propellers in turboprop engines, the sound intensity was lower than the previous state, around 116 decibels. With the increase in the pitch angle, its value increased slightly, but due to the phenomenon of the windmill in the blades, this state cannot be used as reverse thrust. For this reason, similar to the process that will be followed for creating reverse thrust in propeller engines, the engine needs to reduce the rotational speed and the speed of the incoming air. Therefore, the engine speed and speed decreased from 5200 to 3200 rpm and from 660 to 220 km/h, respectively, to create the desired reverse thrust. The sound intensity upstream of the blades in this state is reduced to 82 decibels, and the average sound intensity on the blade surface will be around 132 decibels.

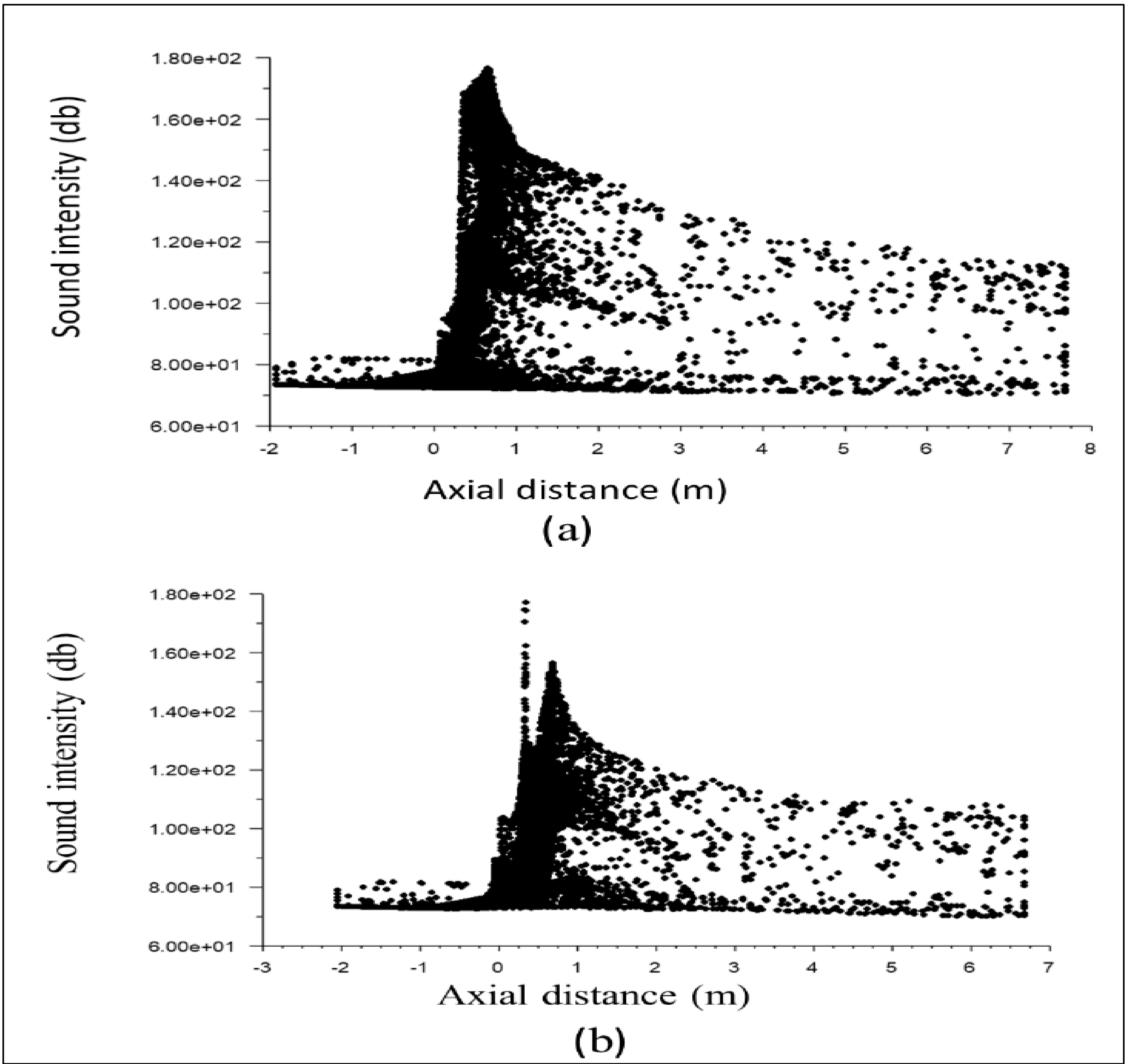

Fig 23 Investigation of Sound Intensity Distribution on the Midsection in the Positive thrust Production State for (a) Reference and (b)Proposed Geometries

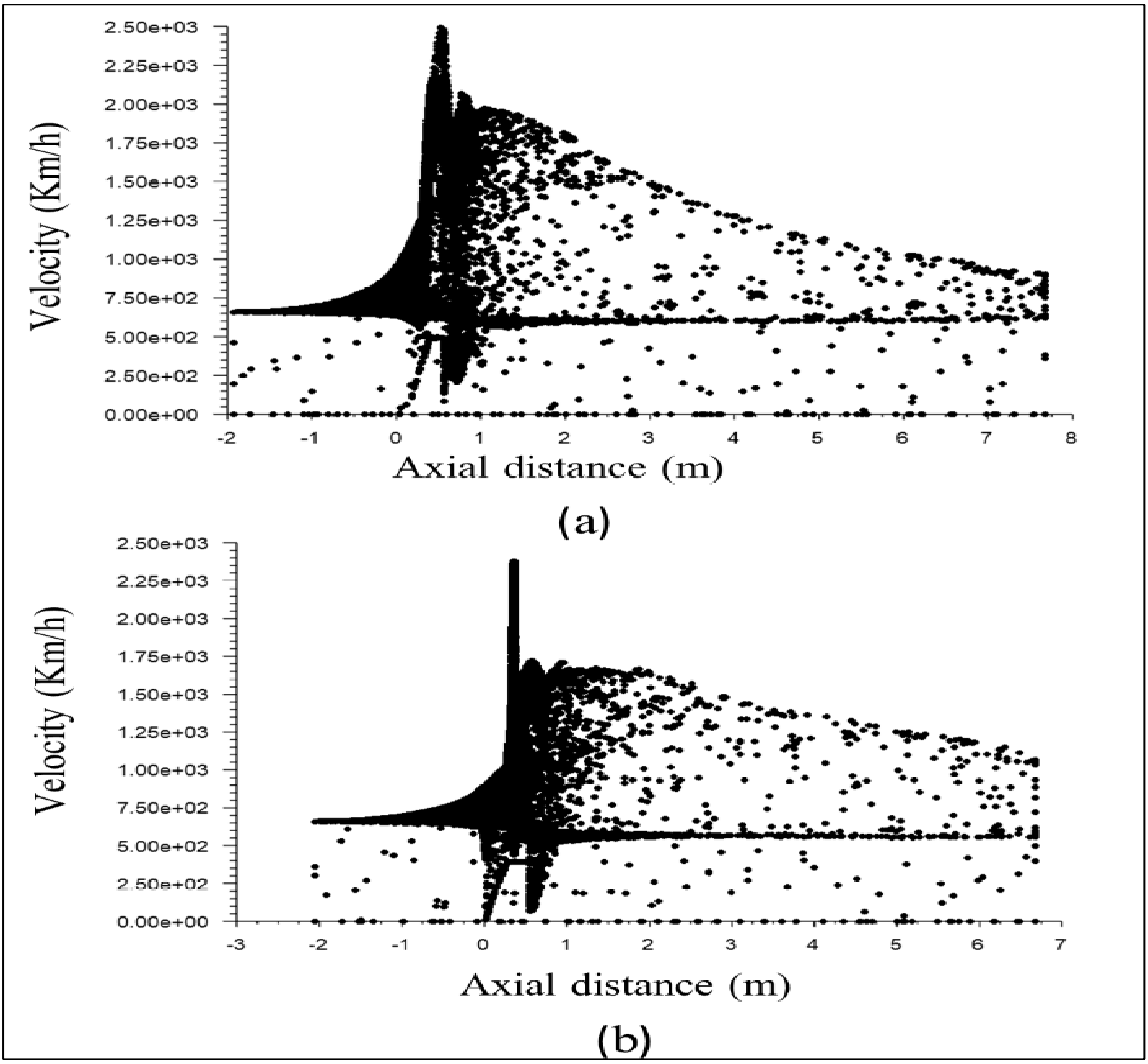

Fig 24 Velocity Distribution Scatter Plots on the Midsection in the Positive thrust Production State for Both the Reference and Proposed Geometries

The results obtained from the simulation of the baseline design showed that the air passing through the CFM56-7B-27 engine fan has an average sound intensity of 118 decibels in front of the blade. However, in this case, the sound intensity of the air behind the blades is higher than up to two meters from the end of the blade and decreases from 170 to 140 decibels with distance from the blade. The average sound intensity of the air behind the nose in this state is 125 decibels on average, which also decreases to 94 decibels with distance from the blade. The upper half of the blade in this state has an average sound intensity of 150 decibels, while in the lower half of the blades, its value decreases to 110 decibels.

In the case where propeller sections were used in the fan design, the results showed that the speed immediately upstream of the blades also increases to 1750 km/h, although in front of the blade at a point with coordinates [3.5 and 0.8 and 0], the air speed will be around 1280 km/h.

The data obtained from the simulation of the CFM56-7B-27 engine fan showed that the air outlet velocity from the blade at the above point is 1230 km/h. Figure 25 shows the velocity distribution at different intersections of both geometries, according to which it is observed that in the second design geometry, considering that the outlet air velocity at a known point is slightly higher than the air velocity passing through the CFM engine fan at that specific point, the air velocity passing over the blade surface and its tip also decreases, which will result in a better result both metallurgically and acoustically at the tip of the blade.

ISSN No:-2456-2165 https://doi.org/10.38124/ijisrt/IJISRT24SEP1537

In the following, after reviewing the sound intensity and velocity, the pressure component in different parts of the computational domain was studied. As shown in Figure 26, it has been observed that in each geometry, based on the theory of the blades, the pressure value on the surface of the blade in the two opposite faces will be different, which is the difference in pressure in the tables and contours have appeared in the form of positive and negative pressures. The results showed that the values of negative pressures will increase. On the other hand, with the presence of positive pressures, which mainly occur at the leading edge of the lower surface of the blades, the amount of pressure difference on the surface of the blades increases and leads to more thrust and momentum in the blade. Therefore, the forces of the most thrust produced.

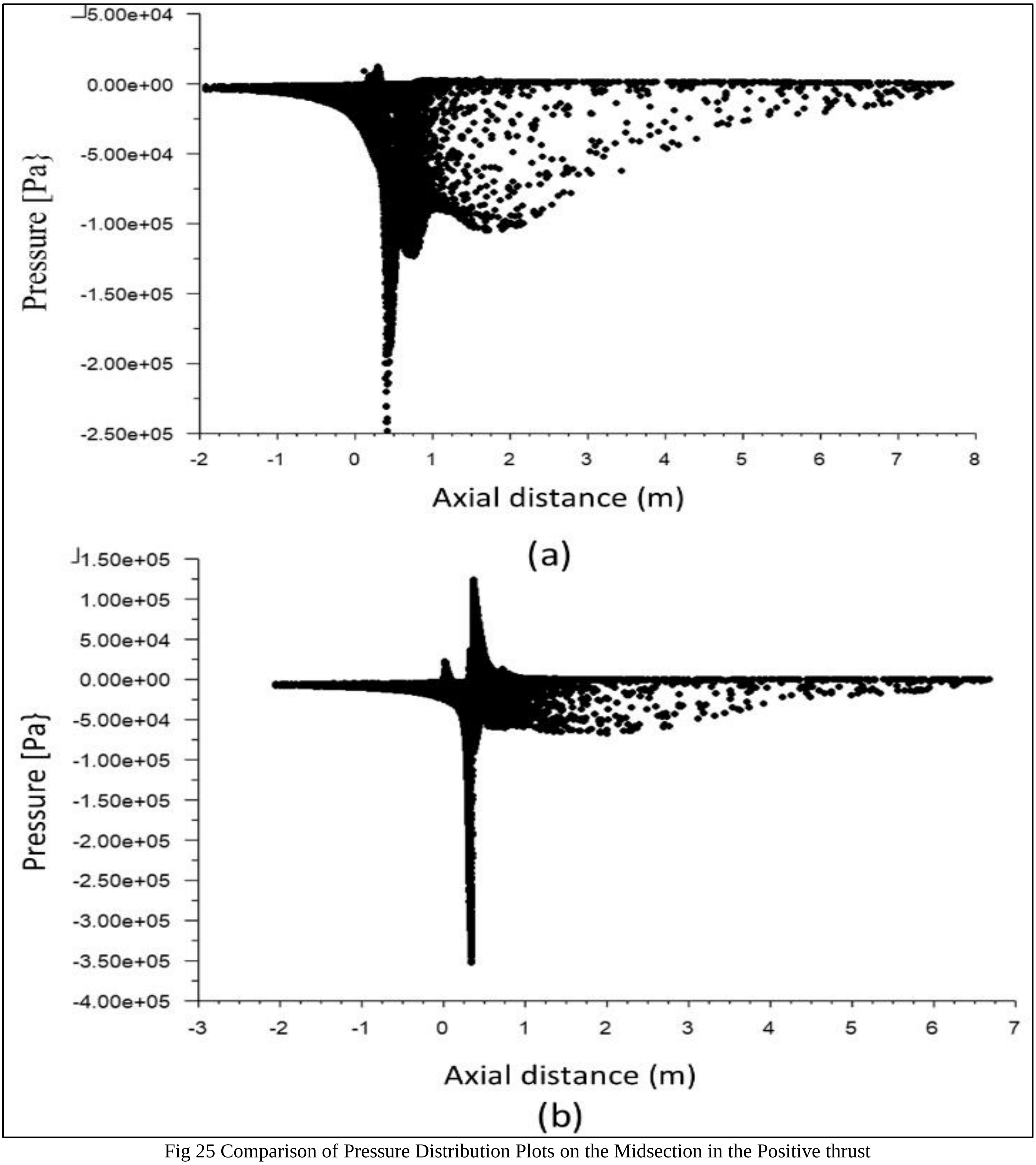

Fig 25 Comparison of Pressure Distribution Plots on the Midsection in the Positive thrust Production State for Both the Reference and Proposed Geometries

ISSN No:-2456-2165 https://doi.org/10.38124/ijisrt/IJISRT24SEP1537

III. CONCLUSION

Despite the remarkable advancements in the manufacturing and development of turbofan engines, one area that has received less attention is reverse thrust technologies in turbofan engines. Although various ideas have been presented for turboprop and jet engines, some designs have proven their merit in generating reverse thrust, leading researchers to put them into practice. In this context, this research aims to investigate an innovative idea for generating reverse thrust in turbofan engines by utilizing co-axial, radial double-row fans. Subsequently, some of the advantages and disadvantages of this idea will be explored to create a new research and development platform for generating reverse thrust in turbofan engines. The data investigated in this research include the pressure, velocity, and sound intensity distributions of the fan blades and the air exiting from it. The thrust produced at each pitch angle in the four proposed geometries was also calculated.

The proposed designs have been designed in three different geometries in SolidWorks software, each with different cross-sections compared to each other in the fan blades. Since the goal of the research is to create reverse thrust by changing the pitch angle, the geometries have been designed and then simulated in ANSYS-Fluent at two or three different pitch angles depending on their design basis. The design process of the blades was based on the knowledge of aerodynamic laws of the blades and the principles of turbomachinery, and then optimized through trial and error to achieve optimal results. After designing and simulating the proposed geometries, a baseline design was created to compare the results obtained from the proposed geometries with the baseline design to assess their merits or shortcomings. This baseline design is based on the CFM56-7B-27 turbofan engine fan, whose geometric information is available through technical manuals and engine guides. In addition, to ensure the accuracy of the design and simulation information, the thrust produced by the baseline design and the actual engine were compared, and the results showed that the thrusts produced were consistent with each other with an error of less than 2%.

In the proposed design geometry, which was designed based on propellers, the amount of positive thrust at the base pitch angle of 12.5 degrees was estimated to be 292,917 kN. The rotational speed of the fan blades and the permissible axial velocity of the incoming air have been reduced to 3200 rpm and 220 km/h, respectively, to prevent the occurrence of the windmill effect on the fan blades, in order to produce a desirable reverse thrust force of 25,077 kN in the opposite direction of the aircraft's movement.

Based on what has been studied in this research, it can be concluded that the use of blades similar to the design geometry under study as the inlet fan of the turbofan engine will bring advantages, including an almost threefold improvement in the generated thrust force, the possibility of generating reverse thrust force when the rotational speed of the blades and the inlet air velocity are reduced compared to the maximum power state, and also a 11% reduction in tip noise.

The research conducted has investigated a geometry of the turbofan engine fan blades that has the ability to change the pitch angle of the blades. The sections of the asymmetrical axial airfoils have been used in this research for a more comprehensive and complete study of the subject, which will be responsible for generating reverse thrust force. Unlike conventional engines, the proposed design includes two-row radial fans, the inner fan (inner fan) is responsible for supplying air to the main and internal components of the engine, while the outer fan blades (second row) will be responsible for generating 80% of the turbofan engine thrust.

Since the study conducted was only theoretical, it requires laboratory results for final confirmation of its effectiveness compared to conventional fans. The research conducted, by simplifying the problem, including ignoring some of the engine components such as the engine frame, inlet guide vanes, and central engine components in the simulation, and also not considering the effects of the materials and alloys used in the blade design, has achieved the above results, which will require a review of all the mentioned parameters for practical implementation and further study in this area.

➢ *Nomenclature:*

- C_L Lift coefficients
- C_D drag coefficients
- ρ air density
- V relative wind speed
- dr width of the blade element
- u velocity
- p pressure
- μ dynamic viscosity
- g gravitational acceleration
- f body forces
- e specific energy
- k thermal conductivity
- T temperature,
- q specific heat flux
- Φ specific energy production due to turbulence
- ω decay rate of energy per unit volume and time
- ∇^2 del represents the Laplace operator
- k a positive number called the wave number
- $\partial^2 P/\partial t^2$ the second derivative of sound pressure with respect to time
- c the speed of sound in the medium
- U blade speed
- θ the angle between the flow direction and the blade axis or the collision or angle of attack
- β pitch angle of the blades from the axis of rotation of the fan.
- c_t the mass quantity coefficient (between 0 and 1)

REFERENCES

[1]. Thrust reversal, wikimedia.orghttps://en.wikipedia.org/wiki/Thrust_reversal
[2]. Boeing 747-400 Mega Splash during thrust reverse, (2016, June 8), Havayolu 101<https://www.havayolu101.com>
[3]. Reemsnyder, D & Sagerser, D. (2012). Effect of forward velocity and crosswind on the reverse-thrust performance of a variable-pitch fan engine. 17th Aerospace Sciences Meeting ,15 January 1979 - 17 January 1979, New Orleans,LA,U.S.A., https://doi.org/10.2514/6.1979-105
[4]. Hall, D. K., & Gunn, E. J. (2014). Aerodynamics of boundary layer ingesting fans. In 33rd AIAA Applied Aerodynamics Conference (p. 3369). American Institute of Aeronautics and Astronautics.
[5]. Moreno, A. C., & Martínez-Val, R. (2012). Performance and noise assessment of counter-rotating turbofan engines. Journal of Aircraft, 49(3), 786-796.
[6]. NASA. (1976). Variable-pitch fan system for NASA/Navy research and technology aircraft (NASA-CR-135185). National Aeronautics and Space Administration.
[7]. Steffen, F. W., McArdle, J. G., & Coats, J. W. (1959). Performance characteristics of hemispherical target-type thrust reversers (NASA Technical Note D-119). National Advisory Committee for Aeronautics.
[8]. Moreno, A. C., & Martínez-Val, R. (2012). Performance and noise assessment of counter-rotating turbofan engines. Journal of Aircraft, 49(3), 786-796.
[9]. Saiyed, N. H., & Bridges, J. E. (2000). Acoustics and thrust of separate-flow exhaust nozzles with mixing devices for high-bypass-ratio engines (NASA/TM-2000-210524). NASA Glenn Research Center.
[10]. Atassi, H. M., & Logue, M. M. (2008). Fan broadband noise prediction for turbofan engines. Journal of Sound and Vibration, 312(4-5), 527-547.
[11]. Rao, J. S., & Sharma, O. P. (2019). Installed flow field of a variable pitch fan operating in reverse thrust. Journal of Engineering for Gas Turbines and Power, 141(7), 071017
[12]. Rao, J. S., & Sharma, O. P. (2020). Rationale for integrated model fidelity to study variable pitch fan reverse thrust. Journal of Engineering for Gas Turbines and Power, 142(5), 051008.
[13]. Rostamalizadeh, H. (2017). Introduction and Analysis to fan blade profile and CFD Simulation Of An Appropriate Blade Profile for improving energy efficiency This. Senior mechanical energy conversion trends. Iran University Of Science and technology(PARDIS).
[14]. Smith, J. D., & Johnson, A. R. (2023). Aerodynamic analysis of wing-engine interference in high-bypass-ratio turbofan engines. Journal of Aerospace Engineering, 36(4), 215-230. https://doi.org/10.1000/aerospace.2023.1234
[15]. Zhang, Y., Zhang, W., & Wang, J. (2021). Numerical simulation of reverser flow field characteristics of business jet during landing process. Aerospace Science and Technology, 110, 106513.
[16]. Mishra, D. P., Sinha, A., & Das, S. K. (2013). Selection of an appropriate aerofoil blade profile for improved performance of axial flow mine ventilation fans using CFD simulations. International Journal of Mining Science and Technology, 23(4), 537-543.
[17]. Varsegov, V. L., & Shabalin, M. V. (2018). Numerical simulation of flow in a cascade-type thrust reverser of a turbofan engine. Russian Aeronautics, 61(4), 556-563.
[18]. Schrantz, P. R. (2015). Variable pitch fan system for high bypass turbofan engines. Journal of Engineering for Gas Turbines and Power, 137(4), 042602.
[19]. Wang, Y., Shen, W., & Xie, H. (2006). A model for the evolution of product families. In ASME 2006 International Design Engineering Technical Conferences and Computers and Information in Engineering Conference (pp. 977-985). American Society of Mechanical Engineers.
[20]. Zhang, X., & Chen, X. (2019). Aerodynamic and acoustic analysis of a cold stream thrust reverser cascade. Aerospace Science and Technology, 94, 105385.